



Online Headspace-Solid Phase Microextraction-Gas Chromatography-Mass Spectrometry-based untargeted volatile metabolomics for studying emerging complex biopesticides: A proof of concept

Hikmat Ghosson, Delphine Raviglione, Marie-Virginie Salvia, Cédric Bertrand

► To cite this version:

Hikmat Ghosson, Delphine Raviglione, Marie-Virginie Salvia, Cédric Bertrand. Online Headspace-Solid Phase Microextraction-Gas Chromatography-Mass Spectrometry-based untargeted volatile metabolomics for studying emerging complex biopesticides: A proof of concept. *Analytica Chimica Acta*, 2020, 1134, pp.58-74. 10.1016/j.aca.2020.08.016 . hal-02926025

HAL Id: hal-02926025

<https://hal.science/hal-02926025>

Submitted on 5 Sep 2022

HAL is a multi-disciplinary open access archive for the deposit and dissemination of scientific research documents, whether they are published or not. The documents may come from teaching and research institutions in France or abroad, or from public or private research centers.

L'archive ouverte pluridisciplinaire **HAL**, est destinée au dépôt et à la diffusion de documents scientifiques de niveau recherche, publiés ou non, émanant des établissements d'enseignement et de recherche français ou étrangers, des laboratoires publics ou privés.



Distributed under a Creative Commons Attribution - NonCommercial - NoDerivatives 4.0 International License

Online Headspace-Solid Phase Microextraction-Gas Chromatography-Mass

Spectrometry-based untargeted volatile metabolomics for studying emerging complex

biopesticides: a proof of concept

Hikmat Ghosson^{1,2,*}, Delphine Raviglione^{1,2}, Marie-Virginie Salvia^{1,2,†}, Cédric Bertrand^{1,2,3,†}

1: PSL Université Paris: EPHE-UPVD-CNRS, USR 3278 CRIOBE, Université de Perpignan, 52 Avenue Paul Alduy, 66860 Perpignan Cedex, France

2: UFR Sciences Exactes et Expérimentales, Université de Perpignan Via Domitia, 52 Avenue Paul Alduy, 66860 Perpignan Cedex, France

3: S.A.S. AkiNaO, Université de Perpignan, 52 Avenue Paul Alduy, 66860 Perpignan Cedex, France

†: Equal Contribution

***: Corresponding author: Hikmat Ghosson**

E-mail addresses: hikmat.ghosson@univ-perp.fr / hikmatghosson@gmail.com

Postal address: USR3278 CRIOBE EPHE-CNRS-UPVD, Bâtiment T, Université de Perpignan, 52 Avenue Paul Alduy, 66860 Perpignan Cedex, France

Tel: +33.6.19.47.12.81

Keywords

Untargeted Metabolomics; Complex biopesticides; Solid Phase Microextraction; Headspace; Gas Chromatography-Mass Spectrometry

Highlights

- A novel online Headspace-Solid Phase Microextraction-Gas Chromatography-Mass Spectrometry-based untargeted metabolomics approach was developed to study the environmental fate of an emerging complex bioherbicide: the *Myrica gale* extract.
- A green, non-destructive automated HS-SPME-GC-MS method was developed and applied for a comparative 38-day kinetics experiment to study the fate of herbicide's volatile xenometabolome after its application on soil samples.
- Untargeted metabolomics and multivariate statistical analyses explained the evolution of herbicide residues over time and allowed for the putative annotation of 96 compounds.
- The approach proved its reliability for high throughput analyses and only required a small number of samples that were not destroyed during the study.

Graphical Abstract

Placed at the end of the manuscript.

Abstract

This work introduces a novel online Headspace-Solid Phase Microextraction-Gas Chromatography-Mass Spectrometry-based untargeted metabolomics approach, suggested as an alternative tool to study the environmental fate of volatile xenometabolites in emerging complex biopesticides, *e.g.* the *Myrica gale* methanolic extract herbicide containing several unknown metabolites. A “living” microcosm sample was designed for non-destructive analysis by a 35-minute HS-SPME automated extraction and a 36-minute GC-MS run. A 38-day kinetics study was then applied on two groups of soil samples: control and spiked. Statistical tools were used for the comparative kinetics study. The Principal Component Analysis revealed and explained the evolution and the dissipation of the herbicide volatile xenometabolome over time. The time-series Heatmap and Multivariate Empirical Bayes Analysis of Variance allowed the prioritization of 101 relevant compounds including 22

degradation by-products. Out of them, 96 xenometabolites were putatively identified. They included 63 compounds that are identified as herbicide components for the first time. The Orthogonal Projections to Latent Structures Discriminant Analysis and its Cross-Validation test were used to assess the total dissipation of the herbicide volatile residues. The reproducibility of the method was also assessed. The highest inter-samples ($n = 3$) Peak Area RSD was 7.75%. The highest inter-samples ($n = 3$) and inter-days ($n = 8$) Retention Time SD were 0.43 sec and 3.44 sec, respectively. The work presents a green, non-laborious and high-throughput approach. It required a small number of environmental samples (6 microcosms) that were analyzed 8 times and were not destroyed during the study.

1. Introduction

Pesticides research, development and production are constantly expanding since these chemicals and agents are essential for several anthropogenic and economic activities (*e.g.* agriculture, food production and protection, disease vectors control). Their development however, faces numerous problems due to their potential impact on human health [1–3] and ecology [4,5]. These issues reinforce the requirement and the importance of prior in-depth studies of their fate, impacts and risks on health and environment. Also, the development of new pesticides of natural origins, known as “biopesticides” or “biocontrol agents” (BA), is one of the suggested alternatives to chemical/synthetic pesticides, as they are presumed to be less harmful for human health and environment. Moreover, their dissipation is likely to be relatively fast [6].

Extracted from plants or different types of microorganisms, these emerging natural products are mostly based on one or several bioactive compounds which usually act in a synergic and/or pleiotropic mode of action. Their complex (bio)chemical nature containing several different and unknown molecules and/or macromolecules is requiring new conceptual and

analytical challenges for the assessment of their transformation and dissipation. The classic concepts of fate assessment, such as the DT50 approach [7], are non-applicable for such types of complex pesticides. These classic targeted approaches are limited to known compounds and molecules. In addition, the DT50 approach does not consider the transformation products (TPs) of the pesticide, in particular the unknown TPs. Additional protocols and approaches are therefore needed in order to assess the pesticide transformation in the environment, and to study the impact of its application on environmental biodiversity.

New analytical proxies were thus suggested as alternative approaches for the emerging complex biopesticides, mainly based on untargeted metabolomics strategies [8,9]. A new approach called Environmental Metabolic Footprinting (EMF) was recently introduced by Patil *et al.* [10] and Salvia *et al.* [11]. This new approach presents the application of the untargeted metabolomics as a universal tool for kinetics studies in order to assess both the fate and impact of different types of complex pesticides. This aims to introduce an integrative concept called “resilience time”.

In the two previous mentioned works [10,11], kinetics studies were performed on an important number of samples by applying destructive Solid-Liquid Extractions (SLE) followed by Liquid Chromatography-Mass Spectrometry (LC-MS) analysis. They were restricted to the solid phase of the environmental matrices (soil and sediments). However, studying the volatile part of the xenometabolome, *i.e.* pesticide compounds and their TPs, is essential for the risk assessment of these emerging biopesticides, and in particular for products based on plant essential oils, which contain an important amount of volatile and semi-volatile organic compounds. The OECD guidelines for the testing of chemicals and their transformation recommend the consideration of the volatile part [12,13]. In fact, studying pesticide volatile residues can provide complementary information to better understand its environmental fate. In addition, pesticide volatile residues screening allows to assess the

exposure risk to pesticide compounds for farmers/workers, insects and plants, as well as the exposure to their TPs that might be more toxic. Therefore, the aim of the present work is to introduce the concept of a new untargeted metabolomics-based approach, dedicated to analyze and study the volatile residues of emerging complex biopesticides applied on environmental matrices, by using online Headspace-Solid Phase Microextraction-Gas Chromatography-Mass Spectrometry (HS-SPME-GC-MS).

HS-SPME is an appropriate technique for volatile organic compounds analysis. It is based on extracting and isolating these analytes from the sample by adsorbing and concentrating them on the layer of a coated fiber. Thus, they can be eventually desorbed and introduced in the analytical instrument with or without the need of extraction solvents [14,15]. Since its introduction in 1989 by Belardi & Pawliszyn [16], the SPME is still being widely developed and extensively used for different types of targeted and untargeted analytical approaches as broadly described by Reyes-Garcés *et al.* [17]. For pesticides research, several works have been reported and were mainly focused on targeted screening and quantification of pesticide residues in different environmental and food matrices [18–20]. Untargeted screening to study the transformation of pesticides and to identify their by-products was also reported, but in a much fewer number of publications [18,21,22].

SPME presents several advantages as a green, non-destructive and cost-effective technique. Its automation provides additional advantages, particularly for metabolomics approaches, mainly by enhancing the robustness and the reproducibility of the applied extraction method. Moreover, reducing the laborious time-consuming manual work and sample preparation steps is essential for high throughput analyses and to minimize errors related to sample handling. Otherwise, as a green non-destructive method, the application of the HS-SPME reduces the number of environmental samples needed, by making it possible to analyze the same sample for several time points, particularly in case of kinetics tracking study. This can also enhance

the performance of the approach by reducing sample preparation and random biological variations-related biases.

On the other hand, GC-MS analytical technique provides several advantages concerning untargeted metabolomics. The GC is a suitable separation technique for volatile and semi-volatile organic compounds. It is well known for its significant analytical robustness, affording high chromatographic resolution and precise retention time repeatability [23]. GC also provides a tool for compounds' identification by allowing the calculation of Kováts Retention Index (RI) [24], which is an advantage for the identification of unknown xenometabolites. Mass spectrometers are highly sensitive detectors capable of characterizing and quantifying compounds. In this work, the chosen detector is a Single Quadrupole MS, equipped with an Electron Impact (EI) ionization system. The main advantages of this spectrometer are the large dynamic range of the Quadrupole mass analyzer, its high scan frequency, and the ability of the EI to provide reproducible fragmentations for the analyzed compounds [23]. This presents an essential tool for characterizing unknown compounds by fast spectral library search and/or by structural elucidation.

All of these advantages were considered for the development of an online HS-SPME-GC-MS method, which was dedicated for studying the environmental fate of an emerging bioherbicide applied on soil: the *Myrica gale* methanolic extract.

Introduced by Popovici *et al.* [25,26], the herbicide composition was partially identified by several studies [25–30]. Its bioactive compound is Myrigalone A, an allelochemical, mixed with several other compounds: mainly triketones and terpenes. The herbicide mode of action was described by Oracz *et al.* [31]. This research work revealed a potential synergic activity between Myrigalone A and terpenes. This activity was recently confirmed and explained by Khaled *et al.* [32]. Therefore, an optimal herbicide activity requires the application of the total

complex mixture of the plant extract. However, several components in this complex mixture are still unknown, and their transformation in nature is not deeply understood. Thus, the untargeted metabolomics approach is a potential solution for studying the environmental fate of this bioherbicide. Therefore, in order to prove the concept of the suggested HS-SPME-GC-MS-based untargeted metabolomics approach, the *Myrica gale* methanolic extract was selected as a typical complex bioherbicide in order to study the dissipation of its volatile residues after its application on soil, through a 38-days kinetics study. The study targets exclusively volatile residues that are spontaneously released to the gas phase above soil (the headspace) during imitated environmental conditions applied to microcosm samples.

2. Material and methods

2.1. Chemicals

Methanol HPLC grade was purchased from VWR International (Fontenay-sous-Bois, France). The dry methanolic extract of *Myrica gale* was prepared as described Popovici *et al.* [25]. The spiking herbicide solution for application on soil samples was prepared at a concentration of 72 mg mL⁻¹ of dry extract dissolved in Methanol (containing 18 mg mL⁻¹ of the bioactive compound Myrigalone A). C7-C30 Saturated Alkanes mix (1000 µg mL⁻¹ of each component in Hexane) was purchased from Sigma-Aldrich (Saint-Quentin-Fallavier, France).

2.2. Soil material

Soil sample was collected from an arable field at the agricultural domain of the “Institut Universitaire de Technologie” (IUT) of Perpignan, France (42°40'55.1"N 2°53'51.2"E). The surface layer (15 cm) of soil was collected on 3 different points separated by 1.5 meter. After collection, the soil was homogenized and passed through a 2 mm sieve. Then, it was stocked in the dark at 4 °C until the experiment. The soil composition analysis and characterization were performed by Arterris Laboratory (Toulouges, France) accredited by the French

Accreditation Committee (Cofrac). Results were the following: 13.9 % of clay, 60.5 % of silt, 25.6 % of sand, 20 % of soil humidity, 1.7 % of organic matter, 0.98 % of organic Carbon, 15.5 meq 100 g⁻¹ cation exchange capacity (CEC), 214 % Ca²⁺/CEC and pH of 8.1 in water. According to the Soil Textural Triangle of the United States Department of Agriculture [33], this soil is classified as a silt loam soil. It was never been contaminated or exposed to herbicides.

2.3. Soil samples set-up

Samples consisted of 6 g of soil weighted in 20 mL HS-SPME vials (Thermo Fisher Scientific, Courtabœuf, France). This weight was optimized in order to keep 2/3 of the vial volume as headspace. After, vials were hermetically closed by a crimped septum, and two 18G×1 ½" (1.2 × 38 mm) Agani[™] needles (Terumo[®], Leuven, Belgium) were implanted on the extremity sides of the septum (Figure A 1 – Appendix A). This is to assure aerobic conditions by allowing air exchange between the internal headspace and the outside. The prepared soil vials were incubated in a GC 401 growth chamber (Nüve, Saracalar, Turkey) for 24 hours before the spiking in order to reestablish the biological and microbial activity. Incubation conditions were 24 hours day/night cycle with alternation of light/dark, 28 °C/18 °C of temperature, and 40 % RH/65 % RH of humidity (Figure A 2 – Appendix A). The soil moisture was maintained at 20 % during the incubation and throughout the experiment, following a standardized environmental protocol implemented and published in previous works [10,34], aiming to assure conditions that are comparable to real environmental cases. The aim of implementing this sample design was to assure a “living system”. As mentioned previously, samples will be used for several kinetic time points, so measures were taken to ensure that they will not be destroyed during the study.

The preparation of herbicide-spiked soil samples was performed by applying the *Myrica gale* methanolic extract with a dose equivalent to 300 µg of the active compound (Myrigalone A) per gram of soil (1.2 mg of dry *Myrica gale* methanolic extract per gram of soil). This corresponds to ten-times the agronomical field dose, following testing guidelines recommendations [12,13] in order to assess their transformation and risks on health and environment in an extreme pollution scenario [34].

2.4. Headspace-Solid Phase Microextraction development

Automated Headspace-Solid Phase Microextraction (HS-SPME) was performed using a TriPlusTM RSHTM autosampler (Thermo Fisher Scientific, Waltham, U.S.). The extraction method was developed by optimizing the following conditions and parameters: the SPME fiber coating, the incubation time, the extraction time, and the extraction temperature. Tests were performed by analyzing herbicide-spiked soil samples (prepared following the protocol described in Section 2.3.)

SPME fiber coating tests were performed by comparing 6 different types of coatings: 100 µm Polydimethylsiloxane (100 µm PDMS, Fused Silica, 23 Ga, Autosampler), 7 µm Polydimethylsiloxane (7 µm PDMS, Fused Silica, 24 Ga, Autosampler), 85 µm Polyacrylate (85 µm PA, Fused Silica, 23 Ga, Autosampler), 65 µm Polydimethylsiloxane/Divinylbenzene (65 µm PDMS/DVB, Stableflex, 23 Ga, Autosampler), 85 µm Carboxen/Polydimethylsiloxane (85 µm CAR/PDMS, Stableflex, 23 Ga, Autosampler), and 50/30 µm Divinylbenzene/Carboxen/Polydimethylsiloxane (50/30 µm DVB/CAR/PDMS, Stableflex, 23 Ga, Autosampler), all purchased from Supelco (Bellefonte, U.S.). Tests were performed by applying the following HS-SPME conditions: 5 min of incubation time, 30 min of extraction time, and 40 °C of extraction temperature.

Next, the duration of sample incubation before the SPME extraction (incubation time) was assessed in order to choose the optimal condition. 3 different incubation times were tested using the selected 50/30 μm DVB/CAR/PDMS fiber: 5 min, 15 min, and 30 min (extraction time: 30 min, extraction temperature: 40 $^{\circ}\text{C}$).

After, the exposure duration of the SPME fiber to the Headspace (extraction time or adsorption time) was assessed. 7 different values were tested: 5 min, 10 min, 20 min, 30 min, 40 min, 50 min and 60 min (incubation time: 5 min, extraction temperature: 40 $^{\circ}\text{C}$, fiber coating: 50/30 μm DVB/CAR/PDMS).

Regarding extraction temperature, 3 values were tested in order to assess the impact of increasing temperature on volatile metabolic profiles. Tested temperatures are the following: 40 $^{\circ}\text{C}$, 60 $^{\circ}\text{C}$, and 80 $^{\circ}\text{C}$ (incubation time: 5 min, extraction time: 30 min, fiber coating: 50/30 μm DVB/CAR/PDMS).

Finally, a dose response curve was applied after adapting optimal conditions. This in order to examine fiber's over-saturation. 6 different herbicide doses were applied on 6 different batches of soil samples (with 3 biological replicates for each dose batch), and then analyzed and compared to control untreated soil samples (3 biological replicates) in order to assess method's detection limit. The 6 applied doses corresponded to: 10^{-3} -time, 10^{-2} -time, 10^{-1} -time, 1-time, 10-times, and 20-times the agronomic field dose of the herbicide.

For all optimization tests and method's application, the incubated sample vial was shaken vigorously throughout the incubation and the extraction procedures in order to enhance the homogenization of sample temperature.

2.5. Gas Chromatography-Mass Spectrometry

Gas Chromatography-Mass Spectrometry analyses were performed on a Focus GC system coupled to an Electron Impact-Single Quadrupole DSQ II Mass Spectrometer (Thermo Fisher

Scientific, Waltham, U.S.; Bremen, Germany). An Agilent J&W DB-5MS GC column was used (length: 30 m, inner diameter: 0.25 mm, film thickness: 0.25 μm , Agilent Technologies, Santa Clara, U.S.). Desorption was performed in Splitless mode for a duration of 1 min at an inlet temperature of 230 $^{\circ}\text{C}$, followed by a 5 min post-injection fiber conditioning at 260 $^{\circ}\text{C}$ in order to prevent fiber carryovers. The 36-min GC run was developed for an optimal compounds separation. It consisted of a 1 mL min^{-1} constant flow method with Helium as carrier gas. The oven temperature was programmed as the following: an initial temperature of 60 $^{\circ}\text{C}$ was held for 1 min, and was then followed by a first ramp of 10 $^{\circ}\text{C min}^{-1}$ in order to reach 100 $^{\circ}\text{C}$. After, a second ramp of 3 $^{\circ}\text{C min}^{-1}$ was applied and held until a temperature of 182 $^{\circ}\text{C}$ was reached. Finally, the last ramp of 25 $^{\circ}\text{C min}^{-1}$ was applied until a temperature of 230 $^{\circ}\text{C}$ was reached. This end temperature was held for 2 min in order to prevent any potential column carryover. GC-MS transfer line temperature was maintained on 240 $^{\circ}\text{C}$ throughout the run.

The MS acquisition method was a Full MS scan for positive ions with an m/z range of 40-400. The scan rate was 5 scans sec^{-1} (2027.11 amu sec^{-1}). The source temperature was set to 250 $^{\circ}\text{C}$ and the applied detector gain was 30000.

2.6. Software and data processing

GC-MS piloting and data acquisition were performed using Xcalibur 3.0.63 (Thermo Fisher Scientific, Waltham, U.S.). Data were acquired in RAW format and then converted to ANDI format (NetCDF) in order to upload and process them using Galaxy Workflow4Metabolomics platform [35–37]. The automated processing workflow used the metaMS package (Galaxy Version 2.1.1) [38] dedicated for GC-MS data. All of its conditions and parameters were published on the platform [39,40]. In brief, a “matchedFilter” algorithm was used for peak piking, with a Full Width at Half Maximum (FWHM) of 5 (Gaussian model peak) [41]. In

addition, GC-MS peaks were considered for peak piking only if: i) their pseudo-spectra contained a minimum of 5 m/z features, ii) if these peaks were present in at least 70 % of samples belonging to a defined condition. Between the different injections/runs, the similarity threshold between peaks pseudo-spectra was set to 0.7, and maximum peak Retention Time (RT) variation was set to 15 sec in order to prevent any potential splitting of a metabolite feature into two different features. After generating the data matrix, statistical analyses were performed using the R-based MetaboAnalyst platform [42–44]. Xcalibur 4.1.31.9 (Thermo Fisher Scientific, Waltham, U.S.) and AMDIS 2.72 (National Institute of Standards and Technology, Gaithersburg, U.S.) were used for the deconvolution of MS spectra and the manual data processing to cross-check the results obtained by the automated processing. Compass DataAnalysis 4.3 (Bruker Daltonik GmbH, Bremen, Germany) was used for EIC peak area integration and for counting molecular features' number. NIST 14 library search for putative identification of compounds was performed using NIST MS Search 2.2 (National Institute of Standards and Technology, Gaithersburg, U.S.). Welch Two Sample T-test for independent means comparison was performed using the R Commander 2.4-2 "Rcmdr" package [45] of R 3.3.3 software.

2.7. Application for a kinetics study

After all analytical conditions were optimized and set-up, a 38-day kinetics tracking study was conducted to prove the concept of the suggested approach. The studied environmental samples consisted of two different groups of soil vials/microcosms (described in the Section 2.3.) with 3 replicates of each: an untreated control soil (UnTr), and an herbicide-spiked soil (MyrN). After spiking, samples were incubated in the growth chamber with the day/night cycle conditions mentioned in Section 2.3., in order to imitate natural conditions for herbicide transformation in soil.

Next, 8 different kinetic time points were analyzed: day 1, day 2, day 3, day 4, day 8, day 17, day 24, and day 38 after spiking. The same soil samples were analyzed by the HS-SPME-GC-MS developed method for all the 8 time points. The order of injections of the different samples was randomized in order to reduce the impact of potential analytical drifts. Blank injections were performed during each time point analysis, by extracting and analyzing the headspace of an empty 20 mL vial using the same HS-SPME-GC-MS method. For Kováts RI calculation, 20 µL of the C7-C30 Alkanes mix solution were introduced to a 20 mL vial, then it was analyzed by applying the same HS-SPME-GC-MS method.

After each analysis, soil microcosms were re-incubated in the growth chamber until the next kinetics time point.

3. Results and discussion

3.1. Headspace-Solid Phase Microextraction optimization

The HS-SPME method was optimized in order to establish a compromise between three major criteria: i) assuring an optimal sensitivity for a wide-range detection of different types of volatile compounds, ii) applying non-destructive conditions to soil samples, iii) preventing an induced volatilization of compounds that are relatively less volatile in the imitated environmental conditions, as the approach targets exclusively volatile residues that are spontaneously released to the gas phase above soil.

For the selection of the SPME fiber coating, Results of tests are shown in Figure A 3 and Table A 1 (Appendix A). PDMS/DVB, DVB/CAR/PDMS and CAR/PDMS showed better results in term of total TIC area and number of molecular features when compared to the 2 PDMS and the PA coatings. In addition, CAR/PDMS fiber coating showed the highest total TIC area and the highest number of molecular features, followed by the DVB/CAR/PDMS, and then the PDMS/DVB.

Nonetheless, performances of PDMS/DVB, DVB/CAR/PDMS and CAR/PDMS coatings were in-depth examined. A data matrix was generated by processing GC-MS raw data of fiber tests (using the same processing method described in Section 2.6.), and then a Heatmap analysis was applied on the dataset. Heatmap (Figure A 4 – Appendix A) shows that PDMS/DVB and CAR/PDMS coatings differ by their specificity for different types of herbicide compounds (as highlighted with yellow boxes in the Figure A 4). However, DVB/CAR/PDMS coating is able to extract simultaneously a part of compounds that are extracted with the PDMS/DVB exclusively, and another part of compounds that are extracted with the CAR/PDMS exclusively (as outlined by the green boxes in the Figure A 4). Therefore, for the current work, the use of the DVB/CAR/PDMS coating is considered as the best compromise between the highest sensitivity and the widest molecular diversity.

Regarding the duration of sample incubation before the SPME extraction (incubation time), Figure A 5 and Table A 2 (Appendix A) show that the increase of incubation time decreases the sensitivity of the method (in term of total TIC area and number of molecular features). This decrease of sensitivity can be hypothetically explained by the accumulation of a higher ratio of water vapor in the headspace. This may prevent the optimal adsorption of some compounds to the SPME fiber, such as L- α -bornyl acetate containing an Ester function, and epi- γ -Eudesmol and α -Terpineol both containing a Hydroxyl function (Table A 3 – Appendix A). Therefore, an incubation time of 5 min was chosen as an optimum for sensitivity.

Concerning the exposure duration of the SPME fiber to the Headspace (extraction time or adsorption time), results in Figure A 6 and Table A 4 (Appendix A) show that a significant difference (in term of total TIC area and number of molecular features) is observed when comparing 5 min, 10 min and 20 min, vs. 30 min, 40 min, 50 min and 60 min. For those last 4 values of extraction time, total TIC areas and numbers of molecular features seem to be no

more evolving. Therefore, a 30 min extraction time was chosen as a compromise between sensitivity and short-time analysis.

Regarding extraction temperature, this parameter is constrained by two problematics: i) the application of relatively high temperatures risks to deteriorate the environmental samples. These risks should be avoided as the current study aims to implement a non-destructive method. ii) As mentioned previously, the scope of the approach is to target exclusively volatile residues that are spontaneously released to the headspace during the imitated environmental conditions. Applying relatively high temperature can provoke an induced volatilization of compounds that are relatively less volatile in those conditions, which should be avoided in order to prevent a conceptual bias. The provocation of this induced volatilization was proved by testing 3 extraction temperatures: 40 °C, 60 °C, and 80 °C. According to results in Figure A 7 and Table A 5 (Appendix A), the increase of extraction temperature led to a decrease in signal for compounds eluted between 40 °C and 130 °C (0 min to 11 min of RT), meanwhile an increase in signal for compounds eluted between 130 °C and 230 °C (11 min to 21 min) was observed. Therefore, beside its destructive aspect, increasing extraction temperature seems to decrease method's sensitivity for the relatively volatile compounds, meanwhile it increases the signal of compounds that are relatively less volatile in environmental conditions.

On the other hand, temperatures below 40 °C were non-applicable in the current work due to problems in stabilizing incubator temperature. This problem risks deteriorating the reproducibility of the extraction. Thus, 40 °C is considered as the optimal compromise for extraction temperature.

To sum up, the optimal HS-SPME conditions applied for the study are the following: 50/30 µm DVB/CAR/PDMS as fiber coating, 5 min of incubation time, 30 min of extraction time,

and 40 °C of extraction temperature. To assess the over-saturation of the fiber with these conditions, a dose response curve was examined. Results in Figure A 8 and Figure A 9 (Appendix A) show that at 20-times the field dose, the Total TIC area and the number of detected molecular features are still increasing. This means that at the optimized HS-SPME conditions, the fiber is not yet over-saturated when analyzing 10-times the field dose (*i.e.* the dose applied for the kinetics study), as the fiber is still able to adsorb higher number and quantity of compounds.

It is worth mentioning that despite the important influence of moisture ratio on the detection of several volatile metabolites, the variation of this parameter is constrained by the complexity of the environmental context. In fact, the moisture ratio fixed at 20 % throughout the current study aims to assure conditions that are comparable to real environmental cases (following previously published protocols [10,34]). Setting a moisture ratio that does not represent the standardized environmental/biochemical conditions question of the study risks to change the abiotic and biotic transformation pathways of xenometabolites during the kinetics study. In addition, the variation of moisture ratio can *de facto* provoke the volatilization of metabolites that are relatively less volatile when the standardized environmental conditions are in-place.

3.2. Herbicide residues detection and low matrix background

After 1 day of spiking, a rich profile of extracted herbicide volatile residues was detected by HS-SPME-GC-MS analysis, as shown in Figure 1. The detected analytes were eluted between 60 °C and 175 °C (1 min to 30 min of RT), presenting a complex volatile fingerprint with several major and minor compounds.

In contrast to the spiked soil, the HS-SPME extract of the untreated control soil samples did not contain an important number of detected compounds (Figure 1). Compared to the blank

GC-MS profiles, there was no significant difference. In both groups, all detected peaks mainly consisted of silicon-derivate compounds. These compounds are probably issued from the bleeding of septum, fiber and/or GC column.

Figure 1: GC-MS chromatograms of HS-SPME extracts after one day of spiking for spiked samples “MyrN” (red), control untreated “UnTr” samples (green) and blanks (grey). For the two sample groups, figures consist of three overlaid chromatograms (TIC) of the three biological replicates. For blanks, two chromatograms of the two analytical replicates are overlaid. Chromatograms were performed with Compass DataAnalysis 4.3 software. The intensity scale is fixed to 3.50E8.

The poor GC-MS profile of the untreated control soil HS-SPME extracts reveals the difficulty in extracting and/or detecting endogenous metabolites originating from soil. Thus, this method is not suitable for studying the impact of the applied herbicide on the soil biodiversity. The advantage, however, is the selectivity of the HS-SPME-GC-MS method to the residues of *Myrica gale* extract in the current study, leading to a low matrix background. This can improve the study of the environmental fate of the herbicide, by enhancing the detection, the quantification and the identification of volatile compounds issued from its xenometabolome, and preventing matrix effects and interferences originating from the matrix.

3.3. Untargeted metabolomics analyses

To prove the concept of the suggested untargeted approach, the 38-day kinetics tracking was performed by applying the HS-SPME-GC-MS analysis on the two groups of samples; the control untreated soil and the soil spiked with the *Myrica gale* extract herbicide (as described in Section 2.7.). After the end of the kinetics tracking and the acquisition of all data, RAW files were converted to ANDI format (NetCDF) and then uploaded on the Galaxy Workflow4Metabolomics platform for data preprocessing (Section 2.6.). The generated data matrix consisted of 64 analyzed samples (24 untreated control samples, 24 spiked samples, and 16 blank injections), and 376 variables. Each of these variables represents a “picked” pseudo-spectrum after it was defined by retention time-based clustering of its m/z fragment ion signals using CAMERA package [38,46]. *In fine*, depending on the applied parameters of

the preprocessing [39], each variable should represent a relevant detected compound (without neglecting the high possibility of considering noise and artefacts). This acquired data matrix was used for the statistical analyses.

3.3.1. Principal Component Analysis

Figure 2: Principal Component Analysis (PCA).
Plot generated using MetaboAnalyst.

First, the Principal Component Analysis (PCA) was applied. All kinetics time points of both untreated control (UnTr) and spiked (MyrN) samples were integrated. The PCA played an important role for understanding the results that were acquired with this approach. It shows that over time, the volatile metabolic profiles of the spiked samples tend to converge with those of the untreated control samples (Figure 2). According to the first principal component axis (PC1), the later kinetics time points, *i.e.* days 17, 24 and 38 after spiking, were more similar to the control profiles in comparison with the earlier kinetics time points. This means that after 17 days of herbicide application, an important dissipation of its xenometabolome had occurred. In fact, the PC1 that explains 81.4 % of variations, consists of the regression of the main features issued from the xenometabolome. This was confirmed by exploring the loadings of the PC1, revealed by the loading plot of the PCA and the Biplot (Figure 3). The 6 most significant features of the PC1 were only present in the extracts of spiked soils as shown in Figure 4. They were more abundant particularly in the earlier kinetics time points, *i.e.* days 1, 2, 3, 4 and 8 after spiking.

Figure 3: Loading plot and Biplot showing correlations between samples and features of the PC1 and the PC2.
Plots generated using MetaboAnalyst.

Another important result regarding the degradation of the herbicide was revealed by the PCA. In fact, a progressive evolution of the volatile profiles of the earlier kinetics time points, *i.e.* from day 1 (T01) to day 8 (T08), was significantly observed on the second principal component axis (PC2). The explanation of this result is that the PC2, which accounts for 7 %

of variations, consists of two main types of volatile xenometabolites: the major herbicide volatile compounds contained in the *Myrica gale* extract, and the volatile degradation by-products issued from herbicide compounds. These two “families” of xenometabolites constituted the two opposed sides of the PC2 as shown in Figure 2. This explanation was confirmed by the loadings of the PC2 (Figure 3). The 6 most significant features of the upper part of the PC2 axis were the compounds of the herbicide. Their highest abundance was at day 1 (T01), and then started to decay over time (Figure 5A). For the 6 features with the highest contributions in variation on the lower part of the PC2 axis, their abundance increased over time, before starting to decay in the later kinetics time points (Figure 5B). Thus, these features represent the by-products issued from the degradation of the herbicide mixture.

Figure 4: Boxplots of features with the highest contributions in variation of PC1. The abundance in the two groups of soil samples and their evolution over time are represented. Boxplots show the null abundance of these features in all control samples (UnTr). The abundance decay over time in spiked samples is also shown (MyrNT01 to MyrNT38, respectively). Features plots are sorted according to the descending order of their PC1 scores (in absolute value), from the left to the right, and then from the top to the bottom. Plots generated using MetaboAnalyst.

Figure 5: Boxplots of features with the highest contributions in variation on the two opposite sides of the PC2. A: Most significant features on the upper part of PC2 axis. Their highest abundance is at day 1 (MyrNT01), and then it starts to decay through time. B: Most significant features on the lower part of PC2 axis. Their abundance increases through time until starting to decay by days 8 and/or 17 (MyrNT08 and/or MyrNT17). All these features show a null intensity in the control samples (UnTr). Features plots are sorted according to the descending order of their PC2 scores (in absolute value), from the left to the right. Plots generated using MetaboAnalyst.

It is worth mentioning that according to PCA, there was no significant difference between volatile profiles of the untreated control samples over time. This proves another advantage of reducing the matrix background, by eliminating soil biochemical evolution factor from analyses. Therefore, tracking and understanding herbicide’s environmental fate are enhanced from a chemical-analytical point of view.

Ultimately, PCA provided a general understanding of the evolution of xenometabolome through the time. In-depth analyses were then conducted to explain this evolution by filtering and tracking xenometabolites over time, in order to identify their nature and to annotate them.

3.3.2. Xenometabolome features prioritization by time-series Heatmap

As mentioned previously, PCA represented a good tool for an overview understanding of xenometabolome evolution through the time. However, only major molecular traces were revealed by this model. In-depth xenometabolome discovery required different statistical tools dedicated to prioritize and filtrate molecular features of the detected volatile xenometabolites. Therefore, a second different statistical analysis was exploited in this work: the time series-based Heatmap.

The time series-based Heatmap considers all features present in the data matrix, in order to visualize the evolution of their abundances over time. Moreover, it performs a clustering in order to group the correlated variables (molecular features), basing on their evolution profiles over the time, and their abundances in the different sample conditions. Thus, it facilitates the “fishing” of features according to their chemical/biochemical nature.

Results of the applied time series-based Heatmap are shown in Figure 6. The Heatmap was applied on all of the kinetics time points (day 1 to day 38) for both untreated control soil and herbicide-spiked soil groups. In this Heatmap, samples were not clustered but sorted according to treatment condition as the first factor, and then according to time evolution as the second. Features however, were clustered without *a priori*, according to the correlation of their abundances between the different samples.

Figure 6: Time series-based Heatmap. Clustering algorithm: Ward, distance measure: Euclidean. Plots generated using MetaboAnalyst.

The clustering of features led to the identification of 4 main zones of interest. Zone A, divided into two sub-zones, A₁ and A₂, consisted of compounds that were only present in the spiked samples. The majority of these features were at their highest level of abundance at day 1 and then started to decay over time. Thus, they are considered as components of the *Myrica gale* extract herbicide. The difference between the two A sub-zones was that in comparison to the

492 A₂ sub-zone features, A₁ sub-zone features presented a higher intensity at the beginning of the
493 kinetics tracking, and their decay over time was faster. A₂ sub-zone features however, had
494 lower intensities at the beginning of the tracking compared to A₁ sub-zone features. They
495 decayed more slowly and some of these features were still present on day 38.

496 Zone B consisted of features that appeared at the middle of the kinetics tracking. Therefore,
497 those features were considered as degradation by-products. Zone C features were also
498 considered as degradation by-products. They appeared at the end of the kinetics tracking,
499 however.

500 Zone D, also divided into two sub-zones, D₁ and D₂, represented features that were abundant
501 in both control and spiked samples. Most of these features were considered as noise and
502 artefacts as they showed a random dispersion of abundances between replicates. For sub-zone
503 D₁, features were identified as random artefacts and noise issued from the complex
504 xenometabolome profile. As this complexity is relatively higher in spiked samples at day 1
505 and day 2, this can explain the reason why this noise is higher in those samples, and less
506 intense in the control samples. For sub-zone D₂ the most relevant of these features were
507 examined by a fast putative annotation using NIST 14 library. All of these features were
508 silicon-derivate compounds. Thus, they were considered as products of septum, fiber and
509 column bleeding. These features were also found in blank injections, which confirmed this
510 hypothesis. It is worth mentioning that the significant features of the D₂ sub-zone were more
511 abundant in the untreated control soil samples. This can be explained by the possible fact that
512 in the spiked samples, the adsorption sites of the SPME fiber were less “available” due to the
513 presence of a rich volatile xenometabolome, bleeding compounds originating from the vial
514 septum were thus less able to fixate on the fiber.

Afterwards, as important numbers of features were prioritized by the Heatmap, a verification procedure was performed in order to filter and remove the eventual hidden artefacts. This procedure was performed using the Multivariate Empirical Bayes Analysis of Variance (MEBA) approach for time series, based on the timecourse method [47], and designed for the comparison of temporal profiles across different conditions or groups of treatments.

3.3.3. *Xenometabolome kinetics tracking and putative compounds identification*

All of the prioritized significant features, revealed by the Heatmap and verified by the MEBA, were manually tracked over time by integrating their GC-MS pseudo-spectra peak areas over all the RAW files. This was done in order to draw their time evolution curves according to the 38-day kinetics tracking. In addition, this manual tracking is recommended in order to crosscheck the automatically generated results and to avoid any false positives that may occur due to the potential errors of the automated data preprocessing.

The manual tracking finally led to consider 101 features as relevant, including 22 features that were considered as degradation by-products according to the kinetics profiles/curves evolution over time. All of these kinetics profiles are shown in Appendix B. Two orthogonal tools were used for putative identification of compounds: the EI-MS fragmentation patterns search on NIST 14 spectral library, and the calculation of Kováts RI that were compared to RI values reported in the NIST library. Kováts RI calculation was performed following the method of Lucero *et al.* [48]. Out of the 101 relevant features, 96 compounds including 20 degradation by-products, representing 99.83 % of the total TIC area after blank subtraction were putatively identified on the levels “2” and “3” of identification confidence according to Sumner *et al.* [49]. The most abundant compounds and all identified degradation by-products are shown in Table 1. Detailed annotations of all the 101 prioritized features are summarized in Table A 6 (Appendix A). Furthermore, out of the 96 annotated compounds, 33 were

reported in the literature as *Myrica gale* essential oil components [28–30]. All of these 33 compounds found in the literature were abundant at day 1 after spiking, representing 67.82 % of the total TIC area after blank subtraction. Meanwhile 63 compounds (47 herbicide components and 16 degradation by-products) are identified for the first time as compounds originating from the *Myrica gale* extract. Figure 7 shows kinetic profiles of the 6 major compounds identified: Eucalyptol, L-terpinen-4-ol, α -Terpineol, α -Terpineol acetate, 3,7(11)-Selinadiene and Germacrone. The rest of the xenometabolites were predominantly terpenes, aromatic and aliphatic esters, alcohol and ketones (Table A 6 – Appendix A).

Figure 7: Kinetic profiles of the 38-day degradation tracking of the 6 major compounds detected. The Peak Areas represent the sum of EICs of the major EI-fragments/ions.

Otherwise, several of the identified degradation by-products could be hypothetically related to the detected *Myrica gale* extract compounds. For instance, Figure 8 shows the kinetics profiles of 2,3-Dehydro-1,8-cineole, Camphor, and Camphene hydrate, that are hypothetically the by-products of Eucalyptol and Borneol after oxidation, and Camphene after hydration, respectively.

Figure 8: Kinetics profiles of the 38-day degradation tracking of the 3 volatile degradation by-products: 2,3-Dehydro-1,8-cineole, Camphor, and Camphene hydrate. The Peak Areas represent the sum of EICs of the major EI-fragments/ions.

It is worth to mention that several degradation by-products (14 out of 22, representing 5.49 % of the total TIC area after blank subtraction), were detected at the day 1 after spiking. This can be explained by three different hypotheses: i) the degradation of their parents was very fast so they started to appear after 1 day of the application of the herbicide, ii) they were already present in the applied herbicide mixture due to a slight degradation of their parents during the extraction and/or the stock of the *Myrica gale* extract, iii) these compounds are not only degradation by-products but also essential components of the *Myrica gale* extract. This last case can be considered for the Camphor and the Camphene hydrate that were reported in the

literature as components of the *Myrica gale* essential oil, as well as their hypothetic parents, *i.e.* Borneol and Camphene, respectively.

Thereby, this fast putative identification, based on fast library search for EI-MS fragmentation spectra and the Kováts RI calculations, presents one of the main advantages of this approach. Indeed, it allowed studying the complex mixture of the emerging natural herbicide, where several of its unknown components and TPs could be putatively identified. The EI fragmentation patterns and their reproducibility allowed the fast annotation of several of these unknown xenometabolites by a simple spectral library search, despite the low resolution of Quadrupole mass analyzer in measuring ions' m/z values. Kováts RI calculations assured higher identification confidence by providing an additional and orthogonal tool for metabolites characterization.

Table 1: Summary of putative identifications of the most relevant features (herbicide xenometabolites with EICs area/total TIC area ≥ 1 %, and identified degradation by-products).

†: The given-code represents the retention time of the compound (in minutes) preceded by the Retention Time "RT" abbreviation.

‡: If $MF \geq 700$, and Δ between experimental and NIST RI ≤ 10 , the considered level of identification confidence is "2". If $MF < 700$, or Δ between experimental and NIST RI > 10 , the considered level of identification confidence is "3" (levels defined by Sumner et al. 2007 [49]).

‡: The percentage of the "sum of major fragments EICs area/total TIC area" ratio, calculated at day 1 after spiking.

N/A: Not Available. N/C: Not Calculated. The relative intensity was not calculated for degradation by-products that were not detected at day 1.

3.3.4. Dissipation assessment by Orthogonal Projections to Latent Structures Discriminant Analysis (OPLS-DA)

Regarding limitations of classic concepts for environmental fate assessment of complex biopesticides, the targeted tracking is not applicable for the present study as described previously. Thus, the comparison of volatile metabolic profiles of both spiked samples and untreated control samples can be considered as an alternative concept to determine the dissipation of volatile compounds of the studied bioherbicide. The total dissipation is considered when the difference between the volatile metabolic profiles of the compared groups is no more significant. Therefore, the choice of the comparative statistical approach

should lay on its ability to reveal the minor differences between the compared profiles. In addition, the significance of those minor differences should be also assessed to avoid the misleading conclusions or the loss of information.

The PCA model is a suitable tool for a holistic overview of the acquired data, as for revealing the major differences. However, minor differences will be hidden and it is difficult to determine them with this descriptive multivariate analysis. Thus, a discriminant analysis is needed for this aim. In this work, Orthogonal Projections to Latent Structures Discriminant Analysis (OPLS-DA) [50,51], and its Cross-Validation (CV) test, were considered to quarry and validate the significance of minor differences that are still present after 38 days of kinetics tracking between spiked samples and control samples.

PCA, OPLS-DA and the CV test of OPLS-DA were applied to compare the volatile metabolic profiles of both spiked soil and untreated control soil samples at day 38 after spiking. This in order to check if the total dissipation of the herbicide has occurred. First, the PCA showed a discrimination between the two conditions according to both PC1 and PC2, explaining 84.9 % and 13.2 % of variations, respectively (Figure A 10 – Appendix A). However, PCA loadings showed that the significance of the two major discriminant features of the PC1 was unreliable, as an important intra-group variation had been noticed (Figure A 11 – Appendix A). Contrariwise, the three major features of the PC2 showed a significant difference between groups (Figure A 11 – Appendix A). Two of those features were considered as persistent xenometabolites as they were not detected in the untreated control samples (RT5.501: o-Cymene and RT1.766: Methyl benzyl sulfoxide). The third feature showing a higher abundance in the untreated control samples was identified as a silicon derivate compound issued from bleeding. It was also detected in the blank injections.

Results of PCA led to conclude that in this descriptive unsupervised multivariate analysis, minor significant discriminations between groups risk to be hidden by the random contaminations and artefacts. Therefore, the OPLS-DA and its CV test were applied as explicative supervised multivariate analyses, in order to reveal significant differences related to the two pre-defined groups (untreated control samples vs. spiked samples). These differences in variables (molecular features) will be revealed by the predictive component (p) of the OPLS-DA. Moreover, the significance of these features will be assessed by introducing the confidence dimension represented by the orthogonal (o) component of the OPLS-DA.

As described in Figure A 12 (Appendix A), the T score shows that the predictive (p) component explains 55.3 % of variations between the volatile profiles of spiked soil and the control soil. The orthogonal component, that explains intra-group variations, represents 16.3 % of variations (Orthogonal T score). Thus, the CV test was performed to assess the significance of “between-groups” and “intra-group” discriminations. The “between-groups” discrimination is assessed by calculating the correlation of samples (R²Y) according to the regressed features of the p component, and by the prediction/significance estimated by the Q² value. The “intra-group” variations are also assessed by calculating the R²Y and Q² applied to the orthogonal component.

The CV test results shown in Appendix A (Figure A 13) were the following: for the p component, R²Y and Q² were 98.7 % and 92.3 %, respectively. For the o component, R²Y and Q² were 1.25 % and 1.94 %, respectively. These results show both R²Y and Q² above 90 %, with R²Y higher than R²X and Q², meaning that the OPLS-DA model is valid. Thus, the discrimination between the two defined groups of samples is significant. In addition, there is a high confidence in the significance of discrimination as the “intra-group” variations were not significant (R²Y and Q² below 50 %, with R²Y lower than R²X and Q²).

Hence, this result means that at day 38 after spiking, the total dissipation of the volatile xenometabolome was not reached. Therefore, to reveal the persistent xenometabolites, the OPLS-DA score plot (S-Plot) can be used as shown in Figure 9. The S-Plot showed several persistent herbicide compounds that were still significantly abundant in the volatile profiles of spiked soil at day 38, *e.g.* RT1.766: Methyl benzyl sulfoxide, RT5.501: o-Cymene, RT25.500: Germacrone, RT20.371: 3,5,11-Eudesmatriene, RT4.333: Methyl 2-methylhexanoate, RT19.447: Calamenene, RT8.073: Camphene hydrate, RT22.148: cis- β -Elemenone. The last 6 mentioned features were difficult to reveal using the PCA loading plot. In addition, the kinetics curves proved coherent results with the S-Plot by showing the persistence of these features after 38 days of herbicide application (Appendix B).

Another advantage of the OPLS-DA S-Plot was its ability to explain the high risk/insignificance of artefacts and contamination features (RT2.671 and RT4.641) previously revealed by the PCA loadings, despite their high contribution in discrimination between groups. This is thanks to the confidence/reliability dimension represented by the $p(\text{corr})[1]$ axis, as explained in Figure 9.

It is worth mentioning that the determination of the total dissipation time of the *Myrica gale* extract herbicide necessitated a longer kinetics study. This however was not in the scope of the present work.

Figure 9: OPLS-DA Score Plot showing the markers of discrimination between the two defined groups of soil samples. The further the feature from the 0 of the $p[1]$ axis, the higher the magnitude of its variation between the two groups. The further the feature from the 0 of the $p(\text{corr})[1]$ axis, the lower its intra-group variation, thus the higher the confidence of its variation significance [52–54]. Plot generated using MetaboAnalyst.

3.4. Repeatability and detection limit assessment

3.4.1. Repeatability

The analytical repeatability of the HS-SPME-GC-MS method was assessed by selecting several important compounds to calculate their Retention Time (RT) and Peak Area (PA)

deviations. The 5 chosen compounds were distributed on the chromatogram RT range (Table 2). “Inter-samples” Peak Area Relative Standard Deviation (RSD) and Retention Time Standard Deviation (SD) were calculated using the 3 biological replicates at the same day (day 1). The highest PA RSD was 7.75 % for the 3,7(11)-Selinadiene, and the highest RT SD was 0.43 sec for Germacrone (Table 2). This proved that the method was highly repeatable. “Inter-days” Retention Time Standard Deviation (SD) was also calculated for the selected compounds using the same sample that was injected 8 times with the following time gaps: 1, 2, 3, 4, 8, 17, 24, 38 days. The highest SD was for the Germacrone with 3.44 sec of deviation (Table 2). “Inter-days” PA variation, however, was not assessed due to the difficulty of the application of Internal Standards (IS) with this type of approach. In fact, as the sample is a living system analyzed for several time points for a period of 38 days, a degradation of IS may occur during the experiment.

Table 2: “Inter-samples” and “inter-days” variations of Peak Area (PA) and Retention Time (RT) over the experiment. “Inter-samples” PA RSD and “inter-samples” RT SD were calculated using the 3 biological replicates. “Inter-days” RT SD was calculated after the same sample was injected 8 times with the following time gaps: 1, 2, 3, 4, 8, 17, 24, 38 days.

3.4.2. Detection limit

As the current study is suggesting an untargeted metabolomics-based approach, classic protocols for targeted method validation are not reasonable (e.g. absolute quantification of targeted compounds using reference standards and calibration curves). Thus, a different concept was applied to assess the detection limit at day 1 of the kinetics study, based on a comparative approximation related to herbicide’s field dose. Untreated control samples were compared to each dose level of the spiked soil samples (described in Section 2.4.). Comparisons were performed using 3 indicators: the Total TIC area integration, the number of the detected molecular features, and by applying OPLS-DA Cross-Validation tests using a data matrix generated after raw data of dose response curve were processed (using the same processing method described in Section 2.6.). Results in Table 3 show that the method is able

to discriminate between the 2 conditions (spiked vs. untreated) from 20-times and until 10^{-1} -time the field dose, as significant differences between the compared conditions are observed for Total TIC areas and for numbers of the detected molecular features (Welch Two Sample T-test p-Values < 5 %), and as a reliable predictivity of the OPLS-DA model is observed for these dose levels (Q^2 of the $p1 > 50$ %). Therefore, a detection limit relative to herbicide dose is estimated between 10^{-1} -time and 10^{-2} -time the field dose at day 1 of the kinetics study.

Table 3: Summary of OPLS-DA CV test and Welch Two Sample T-test results.

3.5. Sample design: a living system after 8 extraction operations

As previously mentioned, the sample design described in Section 2.3. was optimized in order to create a “living system”, such that the same prepared samples (soil vials) could then be tracked by several kinetics time point analyses, as the HS-SPME extraction is a non-destructive method.

After the application of 8 extractions on each vial/sample during the 38-day kinetics study, green plants were observed on top of the soil layer of untreated control samples. The development of this plant layer was progressive during the kinetics study and was even observed 44 days after the end of the kinetics tracking as shown in Figure 10. This indicates that the implemented sample design and the optimized HS-SPME extraction was successful in providing appropriate conditions to sustain a living micro-ecosystem.

Figure 10: The evolution of the untreated control soil vials/microcosms during the experiment. Photo A was taken before the kinetics tracking began. Photo B was taken at the end of the kinetics tracking (at day 38, after analyses). Photos C was taken 44 days after the last time point was analyzed (i.e. after 82 days of the beginning of the kinetics tracking).

4. Conclusion

The present work aimed to introduce a novel HS-SPME-GC-MS-based untargeted metabolomics approach dedicated to study the environmental fate of complex biopesticides. The approach was developed and applied to study the volatile residues of the *Myrica gale*

methanolic extract; an emerging natural herbicide applied to soil, consisting of a complex mixture of identified and non-identified compounds. The developed analytical method was proved reliable in the detection of a rich volatile profile originating from the herbicide, with a low matrix background and a significant robustness. This allowed the fast putative identification of 96 xenometabolites including 33 compounds reported in the literature, 47 compounds identified for the first time as *Myrica gale* extract components, and 16 new degradation by-products, by a 38-day kinetics tracking experiment. A comparison of herbicide-spiked and untreated control soil samples over time demonstrated the advantages of applying the untargeted metabolomics and its statistical tools as an alternative concept for complex pesticides study. The evolution of the herbicide volatile xenometabolome over time can be visualized and explained by using the PCA. The time-series Heatmap method is a suitable tool for prioritizing the relevant xenometabolites and sorting them according to their temporal evolution in the different groups of samples. This is done in order to characterize and identify new xenometabolites and TPs, which can then help to better understand the environmental fate of the herbicide, as well for assessing its potential risk and toxicity on the health and the environment. The OPLS-DA and its CV test provided a sensitive and confident determination of minor discriminations between the different groups of samples in order to assess the total dissipation of the herbicide volatile xenometabolome.

The developed approach successfully revealed all of the significant results and conclusions through an analysis of only 6 environmental samples that were not destroyed throughout the course of the study. Thus, this non-destructive green automated method has now been shown to be capable of cost-effective high throughput analyses. Nevertheless, further analytical and technical developments should be performed to improve the current approach, in order to expand its potential application in environmental fate studies and emerging pesticides research.

Acknowledgments

Authors would like to acknowledge Jeanine Almany (École Pratique des Hautes Études) for providing English language editing (as well as constructing comments) which improved the manuscript. Acknowledgments for Dr. Nicolas Le Yondre (Université de Rennes 1), Dr. Chandrashekhar Patil (Université de Perpignan Via Domitia), and Mathieu Lazarus, M.Sc. (Université de Perpignan Via Domitia) for their scientific and technical advices. Authors also acknowledge two anonymous reviewers for their constructive reviews and critical comments that helped improving the current work.

This work was supported by the French National Research Agency (ANR) under TRICETOX project (ANR-13-CESA-0002), and the European Regional Development Fund (ERDF) under the Interreg POCTEFA PALVIP project (POCTEFA 2014-2020). The funding institutions had no role in the experimental design, the data processing, or in writing and reviewing the manuscript.

Ph.D. fellowship grant was awarded to HG by the French Ministry of Higher Education, Research and Innovation (MESRI), *via* the Doctoral School ED 305 “Energie et Environnement” (Université de Perpignan Via Domitia).

The HS-SPME-GC-MS method developments and analyses had been performed using the Biodiversité et Biotechnologies Marines (Bio2Mar) facilities – Métabolites Secondaires Xénobiotiques Métabolomique Environnementale (MSXM) platform at the Université de Perpignan Via Domitia (<http://bio2mar.obs-banyuls.fr/>).

Authors' contributions

CB, MVS and HG designed the study and edited the draft of the manuscript. HG developed the HS-SPME-GC-MS method, carried out the experimental work and data analyses, and wrote the first and the revised drafts of the manuscript. DR contributed in method's

771 development and instruments' verification and piloting. All authors read and approved the
772 final manuscript.

773 **List of Abbreviations**

774 BA: Biocontrol Agent

775 TP: Transformation Product

776 EMF: Environmental Metabolic Footprinting

777 SLE: Solid-Liquid Extraction

778 LC: Liquid Chromatography

779 MS: Mass Spectrometry

780 OECD: Organization for Economic Co-operation and Development

781 HS: Headspace

782 SPME: Solid Phase Microextraction

783 GC: Gas Chromatography

784 RI: Kováts Retention Index

785 EI: Electron Impact

786 HPLC: High Performance Liquid Chromatography

787 CEC: Cation Exchange Capacity

788 RH: Relative Humidity

789 PDMS: Polydimethylsiloxane

790 PA: Polyacrylate

791 DVB: Divinylbenzene

792 CAR: Carboxen

793 ANDI: Analytical Data Interchange

794 NetCDF: Network Common Data Form

795 FWHM: Full Width at Half Maximum

796 RT: Retention Time

797 EIC: Extracted Ion Chromatogram

798 TIC: Total Ion Chromatogram

799 PCA: Principal Component Analysis

800 PC1: First Principal Component

801 PC2: Second Principal Component

802 MEBA: Multivariate Empirical Bayes Analysis of Variance

803 MF: Matching Factor

804 OPLS-DA: Orthogonal Projections to Latent Structures Discriminant Analysis

805 CV: Cross-Validation

806 S-Plot: Score Plot

807 PA: Peak Area

808 SD: Standard Deviation

809 RSD: Relative Standard Deviation

810 IS: Internal Standard

811 CAS: Chemical Abstracts Service

812 **References**

813 [1] R. McKinlay, J.A. Plant, J.N.B. Bell, N. Voulvoulis, Endocrine disrupting pesticides:
814 Implications for risk assessment, *Environment International*. 34 (2008) 168–183.
815 <https://doi.org/10.1016/j.envint.2007.07.013>.

816 [2] J. Dich, S.H. Zahm, A. Hanberg, H.-O. Adami, Pesticides and cancer, *Cancer Causes*
817 *& Control*. 8 (1997) 420–443. <https://doi.org/10.1023/A:1018413522959>.

818 [3] B.N. Ames, L.S. Gold, Pesticides, Risk, and Applesauce, *Science*. 244 (1989) 755–
819 757. <https://www.jstor.org/stable/1703501>.

820 [4] M. Gavrilescu, Fate of Pesticides in the Environment and its Bioremediation, *Eng.*
821 *Life Sci*. 5 (2005) 497–526. <https://doi.org/10.1002/elsc.200520098>.

822 [5] H.M.G. van der Werf, Assessing the impact of pesticides on the environment,
823 *Agriculture, Ecosystems & Environment*. 60 (1996) 81–96. [https://doi.org/10.1016/S0167-](https://doi.org/10.1016/S0167-8809(96)01096-1)
824 [8809\(96\)01096-1](https://doi.org/10.1016/S0167-8809(96)01096-1).

825 [6] C. Bertrand, C. Prigent-Combaret, A. Gonzales-Coloma, Chemistry, activity, and
826 impact of plant biocontrol products, *Environ Sci Pollut Res*. 25 (2018) 29773–29774.
827 <https://doi.org/10.1007/s11356-018-3209-2>.

828 [7] European Food Safety Authority, EFSA Guidance Document for evaluating laboratory
829 and field dissipation studies to obtain DegT50 values of active substances of plant protection
830 products and transformation products of these active substances in soil, *EFSA Journal*. 12
831 (2014) 3662. <https://doi.org/10.2903/j.efsa.2014.3662>.

- 832 [8] K.A. Aliferis, M. Chrysai-Tokousbalides, Metabolomics in pesticide research and
833 development: review and future perspectives, *Metabolomics*. 7 (2011) 35–53.
834 <https://doi.org/10.1007/s11306-010-0231-x>.
- 835 [9] M.R. Viant, U. Sommer, Mass spectrometry based environmental metabolomics: a
836 primer and review, *Metabolomics*. 9 (2013) 144–158. [https://doi.org/10.1007/s11306-012-](https://doi.org/10.1007/s11306-012-0412-x)
837 [0412-x](https://doi.org/10.1007/s11306-012-0412-x).
- 838 [10] C. Patil, C. Calvayrac, Y. Zhou, S. Romdhane, M.-V. Salvia, J.-F. Cooper, F.E.
839 Dayan, C. Bertrand, Environmental Metabolic Footprinting: A novel application to study the
840 impact of a natural and a synthetic β -triketone herbicide in soil, *Science of The Total*
841 *Environment*. 566–567 (2016) 552–558. <https://doi.org/10.1016/j.scitotenv.2016.05.071>.
- 842 [11] M.-V. Salvia, A. Ben Jrad, D. Raviglione, Y. Zhou, C. Bertrand, Environmental
843 Metabolic Footprinting (EMF) vs. half-life: a new and integrative proxy for the discrimination
844 between control and pesticides exposed sediments in order to further characterise pesticides’
845 environmental impact, *Environ Sci Pollut Res*. 25 (2018) 29841–29847.
846 <https://doi.org/10.1007/s11356-017-9600-6>.
- 847 [12] OECD, Test No. 307: Aerobic and Anaerobic Transformation in Soil, 2002.
848 <https://doi.org/10.1787/9789264070509-en>.
- 849 [13] OECD, Test No. 308: Aerobic and Anaerobic Transformation in Aquatic Sediment
850 Systems, 2002. <https://doi.org/10.1787/9789264070523-en>.
- 851 [14] J. Pawliszyn, *Handbook of Solid Phase Microextraction*, First Edition, Elsevier, 2012.
852 <https://doi.org/10.1016/C2011-0-04297-7>.
- 853 [15] J. Pawliszyn, Theory of Solid-Phase Microextraction, *Journal of Chromatographic*
854 *Science*. 38 (2000) 270–278. <https://doi.org/10.1093/chromsci/38.7.270>.

855 [16] R.P. Belardi, J.B. Pawliszyn, The Application of Chemically Modified Fused Silica
 856 Fibers in the Extraction of Organics from Water Matrix Samples and their Rapid Transfer to
 857 Capillary Columns, *Water Quality Research Journal*. 24 (1989) 179–191.
 858 <https://doi.org/10.2166/wqrj.1989.010>.

859 [17] N. Reyes-Garcés, E. Gionfriddo, G.A. Gómez-Ríos, Md.N. Alam, E. Boyacı, B.
 860 Bojko, V. Singh, J. Grandy, J. Pawliszyn, Advances in Solid Phase Microextraction and
 861 Perspective on Future Directions, *Analytical Chemistry*. 90 (2018) 302–360.
 862 <https://doi.org/10.1021/acs.analchem.7b04502>.

863 [18] M. Llompart, M. Celeiro, C. García-Jares, T. Dagnac, Environmental applications of
 864 solid-phase microextraction, *TrAC Trends in Analytical Chemistry*. 112 (2019) 1–12.
 865 <https://doi.org/10.1016/j.trac.2018.12.020>.

866 [19] D. Liang, W. Liu, R. Raza, Y. Bai, H. Liu, Applications of solid-phase micro-
 867 extraction with mass spectrometry in pesticide analysis, *Journal of Separation Science*. 42
 868 (2019) 330–341. <https://doi.org/10.1002/jssc.201800804>.

869 [20] J. Beltran, F.J. López, F. Hernández, Solid-phase microextraction in pesticide residue
 870 analysis, *Journal of Chromatography A*. 885 (2000) 389–404. [https://doi.org/10.1016/S0021-](https://doi.org/10.1016/S0021-9673(00)00142-4)
 871 [9673\(00\)00142-4](https://doi.org/10.1016/S0021-9673(00)00142-4).

872 [21] J.L. Martínez Vidal, P. Plaza-Bolaños, R. Romero-González, A. Garrido Frenich,
 873 Determination of pesticide transformation products: A review of extraction and detection
 874 methods, *Journal of Chromatography A*. 1216 (2009) 6767–6788.
 875 <https://doi.org/10.1016/j.chroma.2009.08.013>.

876 [22] V. Andreu, Y. Picó, Determination of pesticides and their degradation products in soil:
 877 critical review and comparison of methods, *TrAC Trends in Analytical Chemistry*. 23 (2004)
 878 772–789. <https://doi.org/10.1016/j.trac.2004.07.008>.

879 [23] M. Bedair, L.W. Sumner, Current and emerging mass-spectrometry technologies for
 880 metabolomics, TrAC Trends in Analytical Chemistry. 27 (2008) 238–250.
 881 <https://doi.org/10.1016/j.trac.2008.01.006>.

882 [24] L.S. Ettre, The Kováts Retention Index System, Anal. Chem. 36 (1964) 31A–41A.
 883 <https://doi.org/10.1021/ac60214a727>.

884 [25] J. Popovici, C. Bertrand, D. Jacquemoud, F. Bellvert, M.P. Fernandez, G. Comte, F.
 885 Piola, An Allelochemical from *Myrica gale* with Strong Phytotoxic Activity against Highly
 886 Invasive *Fallopia x bohemica* Taxa, Molecules. 16 (2011) 2323–2333.
 887 <https://doi.org/10.3390/molecules16032323>.

888 [26] J. Popovici, C. Bertrand, G. Comte, Use of a *Myrica gale* plant for producing a
 889 herbicide agent, US008734858B2, 2014. <https://patents.google.com/patent/US8734858B2/en>.

890 [27] J. Popovici, G. Comte, E. Bagnarol, N. Alloisio, P. Fournier, F. Bellvert, C. Bertrand,
 891 M.P. Fernandez, Differential Effects of Rare Specific Flavonoids on Compatible and
 892 Incompatible Strains in the *Myrica gale*-*Frankia* Actinorhizal Symbiosis, Applied and
 893 Environmental Microbiology. 76 (2010) 2451–2460. <https://doi.org/10.1128/AEM.02667-09>.

894 [28] J. Popovici, C. Bertrand, E. Bagnarol, M.P. Fernandez, G. Comte, Chemical
 895 composition of essential oil and headspace-solid microextracts from fruits of *Myrica gale* L.
 896 and antifungal activity, Natural Product Research. 22 (2008) 1024–1032.
 897 <https://doi.org/10.1080/14786410802055568>.

898 [29] K.P. Svoboda, A. Inglis, J. Hampson, B. Galambosi, Y. Asakawa, Biomass
 899 production, essential oil yield and composition of *Myrica gale* L. harvested from wild
 900 populations in Scotland and Finland, Flavour and Fragrance Journal. 13 (1998) 6.
 901 [https://doi.org/10.1002/\(SICI\)1099-1026\(199811/12\)13:6<367::AID-FFJ724>3.0.CO;2-M](https://doi.org/10.1002/(SICI)1099-1026(199811/12)13:6<367::AID-FFJ724>3.0.CO;2-M).

902 [30] R.R. Carlton, P.G. Waterman, A.I. Gray, Variation of leaf gland volatile oil within a
 903 population of sweet gale (*Myrica gale*) (Myricaceae), *Chemoecology*. 3 (1992) 45–54.
 904 <https://doi.org/10.1007/BF01261456>.

905 [31] K. Oracz, A. Voegelé, D. Tarkowská, D. Jacquemoud, V. Turečková, T. Urbanová, M.
 906 Strnad, E. Sliwinska, G. Leubner-Metzger, Myrigalone A Inhibits *Lepidium sativum* Seed
 907 Germination by Interference with Gibberellin Metabolism and Apoplastic Superoxide
 908 Production Required for Embryo Extension Growth and Endosperm Rupture, *Plant and Cell*
 909 *Physiology*. 53 (2012) 81–95. <https://doi.org/10.1093/pcp/pcr124>.

910 [32] A. Khaled, M. Sleiman, E. Darras, A. Trivella, C. Bertrand, N. Inguibert, P. Goupil,
 911 C. Richard, Photodegradation of Myrigalone A, an Allelochemical from *Myrica gale* :
 912 Photoproducts and Effect of Terpenes, *J. Agric. Food Chem.* 67 (2019) 7258–7265.
 913 <https://doi.org/10.1021/acs.jafc.9b01722>.

914 [33] United States Natural Resources Conservation Service - Soil Science Division, Soil
 915 Survey Manual, revised, United States Department of Agriculture, 2017.
 916 <https://books.google.fr/books?id=dieUtAEACAAJ>.

917 [34] S. Romdhane, M. Devers-Lamrani, J. Beguet, C. Bertrand, C. Calvayrac, M.-V.
 918 Salvia, A.B. Jrad, F.E. Dayan, A. Spor, L. Barthelmebs, F. Martin-Laurent, Assessment of the
 919 ecotoxicological impact of natural and synthetic β -triketone herbicides on the diversity and
 920 activity of the soil bacterial community using omic approaches, *Science of The Total*
 921 *Environment*. 651 (2019) 241–249. <https://doi.org/10.1016/j.scitotenv.2018.09.159>.

922 [35] Galaxy Workflow4Metabolomics, Galaxy Workflow4Metabolomics. (n.d.).
 923 <https://galaxy.workflow4metabolomics.org/> (accessed February 28, 2020).

924 [36] F. Giacomoni, G. Le Corguille, M. Monsoor, M. Landi, P. Pericard, M. Petera, C.
 925 Duperier, M. Tremblay-Franco, J.-F. Martin, D. Jacob, S. Goulitquer, E.A. Thevenot, C.

926 Caron, Workflow4Metabolomics: a collaborative research infrastructure for computational
 927 metabolomics, *Bioinformatics*. 31 (2015) 1493–1495.
 928 <https://doi.org/10.1093/bioinformatics/btu813>.

929 [37] Y. Guitton, M. Tremblay-Franco, G. Le Corguillé, J.-F. Martin, M. Pétéra, P. Roger-
 930 Mele, A. Delabrière, S. Goulitquer, M. Monsoor, C. Duperier, C. Canlet, R. Servien, P.
 931 Tardivel, C. Caron, F. Giacomoni, E.A. Thévenot, Create, run, share, publish, and reference
 932 your LC–MS, FIA–MS, GC–MS, and NMR data analysis workflows with the
 933 Workflow4Metabolomics 3.0 Galaxy online infrastructure for metabolomics, *The*
 934 *International Journal of Biochemistry & Cell Biology*. 93 (2017) 89–101.
 935 <https://doi.org/10.1016/j.biocel.2017.07.002>.

936 [38] R. Wehrens, G. Weingart, F. Mattivi, metaMS: An open-source pipeline for GC–MS-
 937 based untargeted metabolomics, *Journal of Chromatography B*. 966 (2014) 109–116.
 938 <https://doi.org/10.1016/j.jchromb.2014.02.051>.

939 [39] H. Ghosson, D. Raviglione, M.-V. Salvia, C. Bertrand, Online HS-SPME-GC-MS-
 940 based untargeted volatile metabolomics for studying emerging complex biopesticides: a proof
 941 of concept - W4M workflow and parameters, *Galaxy Workflow4Metabolomics*. (2020).
 942 [https://galaxy.workflow4metabolomics.org/u/hghosson/w/online-hs-spme-gc-ms-based-](https://galaxy.workflow4metabolomics.org/u/hghosson/w/online-hs-spme-gc-ms-based-untargeted-metabolomics-for-emerging-complex-biopesticides-study-can-we-footprint-the-volatilome)
 943 [untargeted-metabolomics-for-emerging-complex-biopesticides-study-can-we-footprint-the-](https://galaxy.workflow4metabolomics.org/u/hghosson/w/online-hs-spme-gc-ms-based-untargeted-metabolomics-for-emerging-complex-biopesticides-study-can-we-footprint-the-volatilome)
 944 [volatilome](https://galaxy.workflow4metabolomics.org/u/hghosson/w/online-hs-spme-gc-ms-based-untargeted-metabolomics-for-emerging-complex-biopesticides-study-can-we-footprint-the-volatilome) (accessed February 28, 2020).

945 [40] H. Ghosson, D. Raviglione, M.-V. Salvia, C. Bertrand, Online HS-SPME-GC-MS-
 946 based untargeted volatile metabolomics for studying emerging complex biopesticides: a proof
 947 of concept - W4M data, *Galaxy Workflow4Metabolomics*. (2020).
 948 [https://galaxy.workflow4metabolomics.org/u/hghosson/h/online-hs-spme-gc-ms-based-](https://galaxy.workflow4metabolomics.org/u/hghosson/h/online-hs-spme-gc-ms-based-untargeted-metabolomics-for-emerging-complex-biopesticides-study-can-we-footprint-the-volatilome)

949 [untargeted-metabolomics-for-emerging-complex-biopesticides-study-can-we-footprint-the-](#)
950 [volatilome](#) (accessed February 28, 2020).

951 [41] C.A. Smith, E.J. Want, G. O'Maille, R. Abagyan, G. Siuzdak, XCMS: Processing
952 Mass Spectrometry Data for Metabolite Profiling Using Nonlinear Peak Alignment,
953 Matching, and Identification, *Anal. Chem.* 78 (2006) 779–787.
954 <https://doi.org/10.1021/ac051437y>.

955 [42] MetaboAnalyst, MetaboAnalyst. (n.d.). <https://www.metaboanalyst.ca/> (accessed
956 February 28, 2020).

957 [43] J. Chong, D.S. Wishart, J. Xia, Using MetaboAnalyst 4.0 for Comprehensive and
958 Integrative Metabolomics Data Analysis, *Current Protocols in Bioinformatics*. 68 (2019) e86.
959 <https://doi.org/10.1002/cpbi.86>.

960 [44] J. Chong, O. Soufan, C. Li, I. Caraus, S. Li, G. Bourque, D.S. Wishart, J. Xia,
961 MetaboAnalyst 4.0: towards more transparent and integrative metabolomics analysis, *Nucleic*
962 *Acids Research*. 46 (2018) W486–W494. <https://doi.org/10.1093/nar/gky310>.

963 [45] J. Fox, The R Commander: A Basic-Statistics Graphical User Interface to R, *Journal*
964 *of Statistical Software*. 14 (2005) 1–42. <https://doi.org/10.18637/jss.v014.i09>.

965 [46] C. Kuhl, R. Tautenhahn, C. Böttcher, T.R. Larson, S. Neumann, CAMERA: An
966 Integrated Strategy for Compound Spectra Extraction and Annotation of Liquid
967 Chromatography/Mass Spectrometry Data Sets, *Anal. Chem.* 84 (2012) 283–289.
968 <https://doi.org/10.1021/ac202450g>.

969 [47] Y.C. Tai, T.P. Speed, A multivariate empirical Bayes statistic for replicated
970 microarray time course data, *Ann. Statist.* 34 (2006) 2387–2412.
971 <https://doi.org/10.1214/009053606000000759>.

972 [48] M. Lucero, R. Estell, M. Tellez, E. Fredrickson, A retention index calculator simplifies
 973 identification of plant volatile organic compounds, *Phytochemical Analysis*. 20 (2009) 378–
 974 384. <https://doi.org/10.1002/pca.1137>.

975 [49] L.W. Sumner, A. Amberg, D. Barrett, M.H. Beale, R. Beger, C.A. Daykin, T.W.-M.
 976 Fan, O. Fiehn, R. Goodacre, J.L. Griffin, T. Hankemeier, N. Hardy, J. Harnly, R. Higashi, J.
 977 Kopka, A.N. Lane, J.C. Lindon, P. Marriott, A.W. Nicholls, M.D. Reily, J.J. Thaden, M.R.
 978 Viant, Proposed minimum reporting standards for chemical analysis: Chemical Analysis
 979 Working Group (CAWG) Metabolomics Standards Initiative (MSI), *Metabolomics*. 3 (2007)
 980 211–221. <https://doi.org/10.1007/s11306-007-0082-2>.

981 [50] J. Trygg, S. Wold, Orthogonal projections to latent structures (O-PLS), J.
 982 *Chemometrics*. 16 (2002) 119–128. <https://doi.org/10.1002/cem.695>.

983 [51] H. Wold, Estimation of principal components and related models by iterative least
 984 squares, in: *Multivariate Analysis*, Krishnaiah, P. R., Academic Press, 1966: pp. 391–420.
 985 <https://ci.nii.ac.jp/naid/20001378860/en/>.

986 [52] J. Cohen, Things I have learned (so far)., *American Psychologist*. 45 (1990) 1304–
 987 1312. <https://doi.org/10.1037/0003-066X.45.12.1304>.

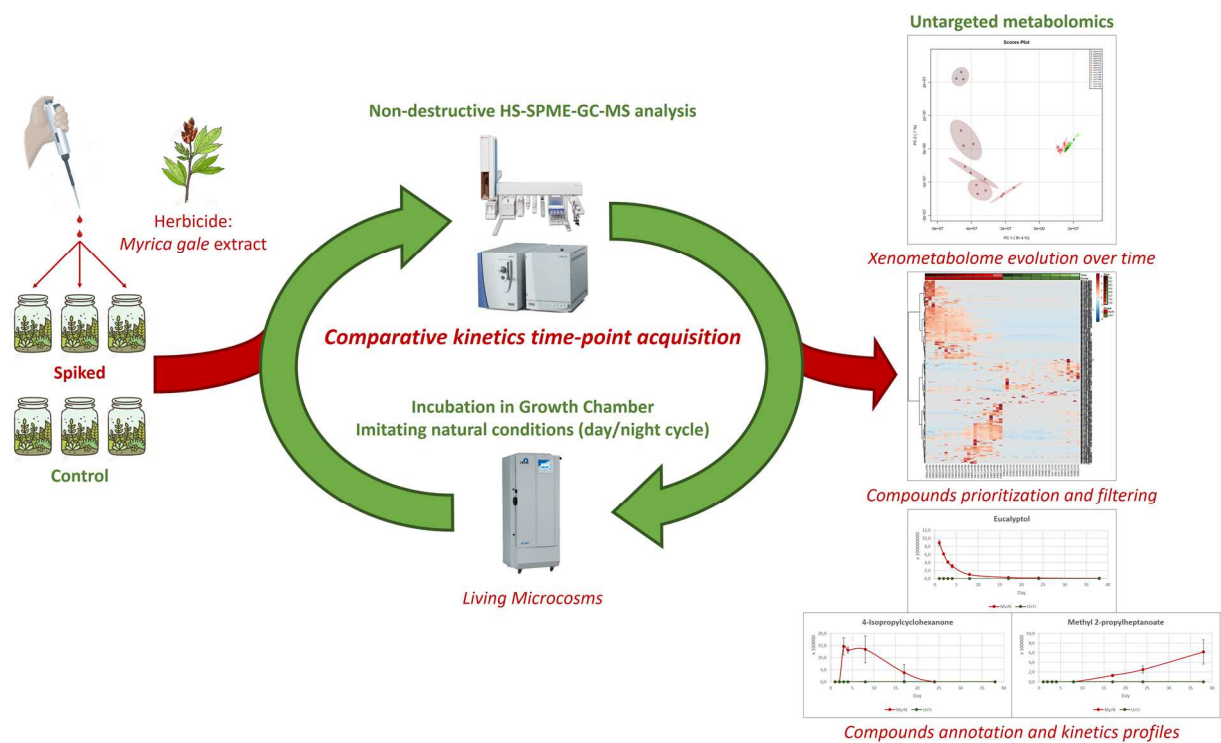
988 [53] A. Roux, Analysis of human urinary metabolome by liquid chromatography coupled
 989 to high resolution mass spectrometry, Theses, Université Pierre et Marie Curie - Paris VI,
 990 2011. <https://tel.archives-ouvertes.fr/tel-00641529>.

991 [54] S. Wiklund, Multivariate data analysis for Omics, (2008).
 992 https://metabolomics.se/Courses/MVA/MVA%20in%20Omics_Handouts_Exercises_Solutions_Thu-Fri.pdf.

994

995

996



997

998

Graphical Abstract

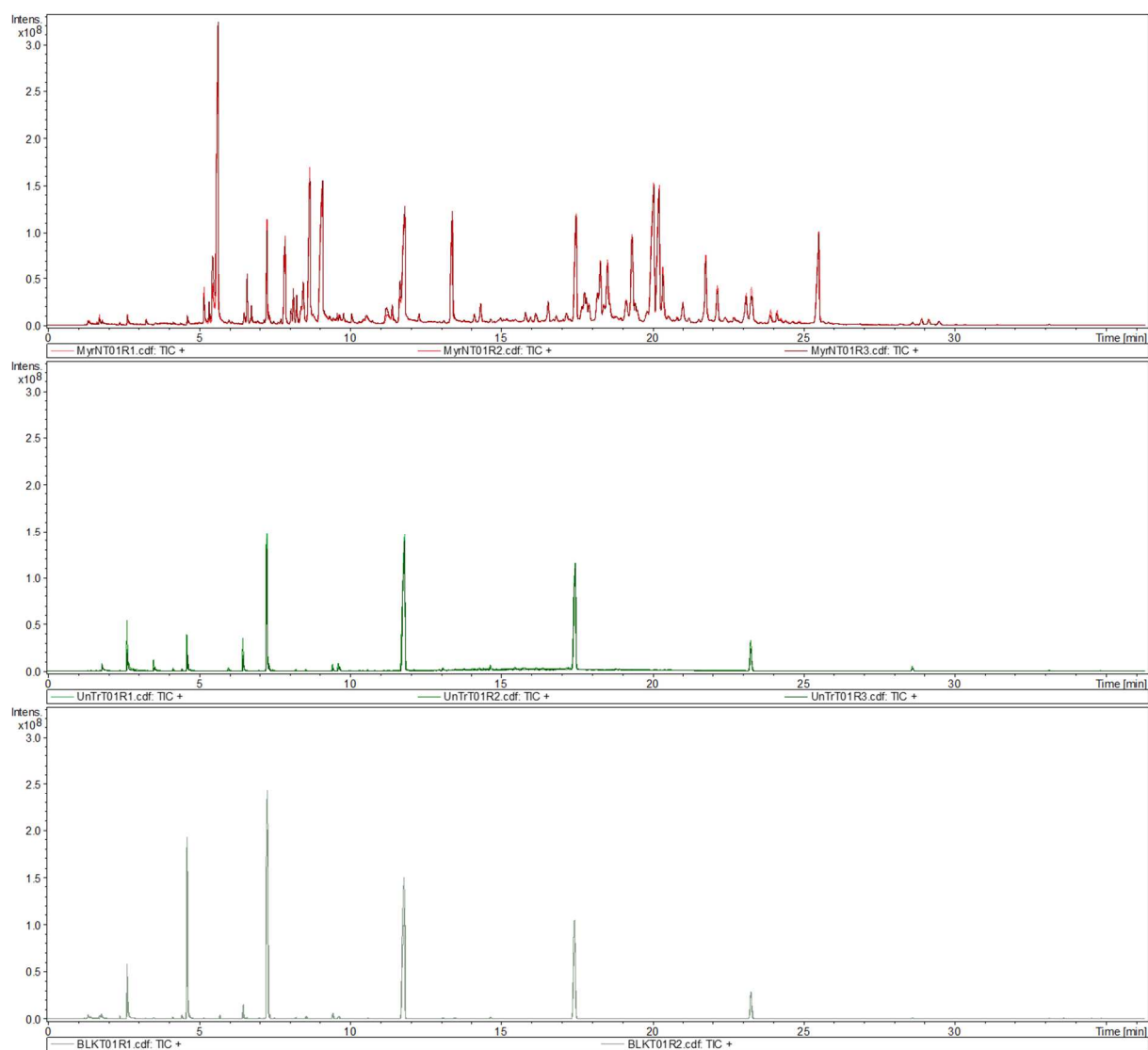
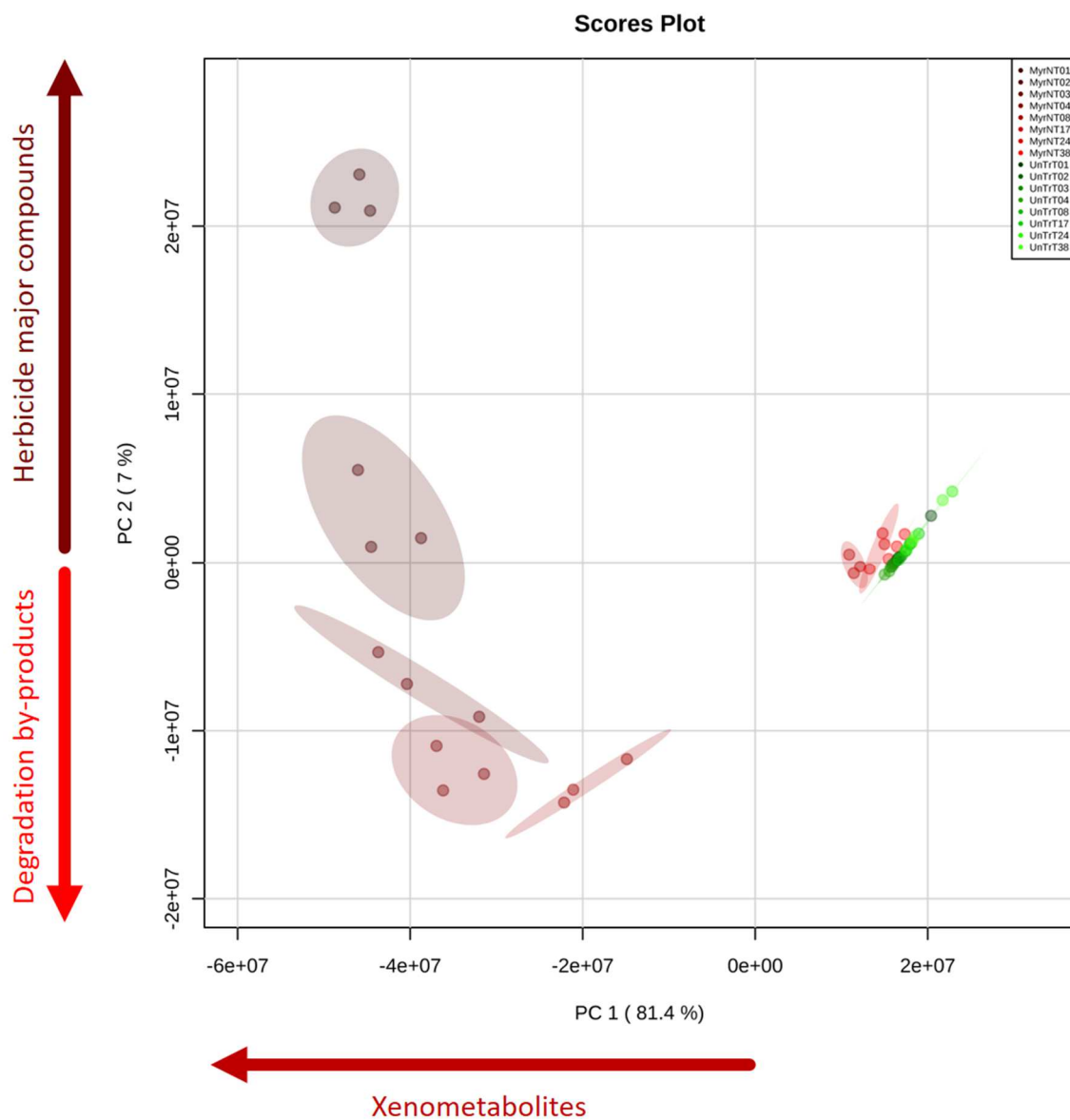


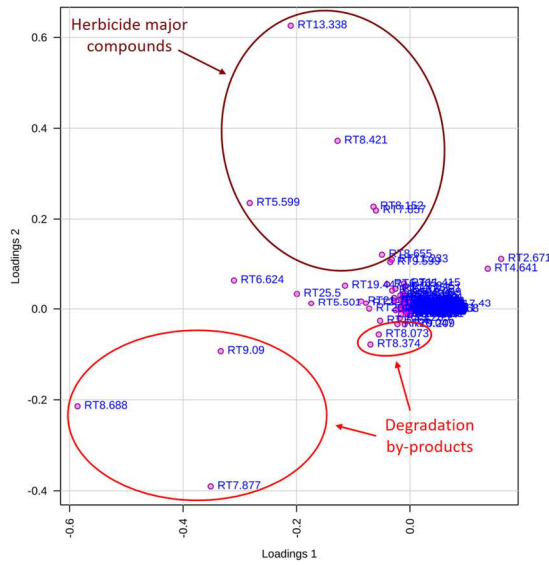
Figure 1



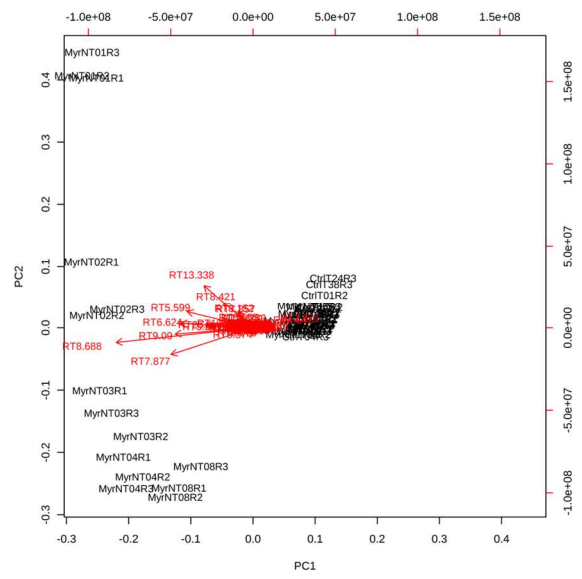
1001

1002

Figure 2



a: PC1 × PC2 Loading plot



b: PC1 × PC2 Biplot

Figure 3

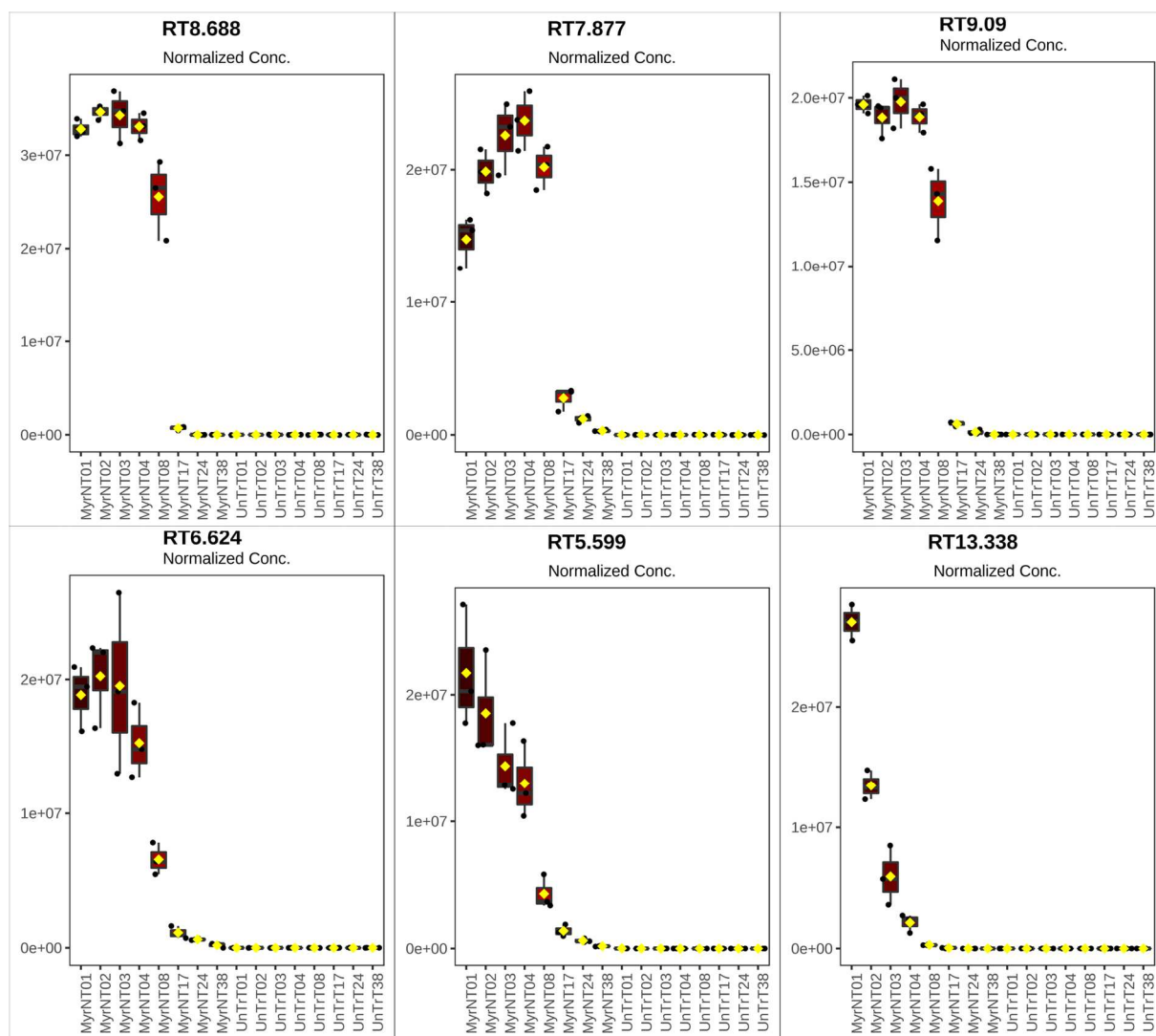


Figure 4

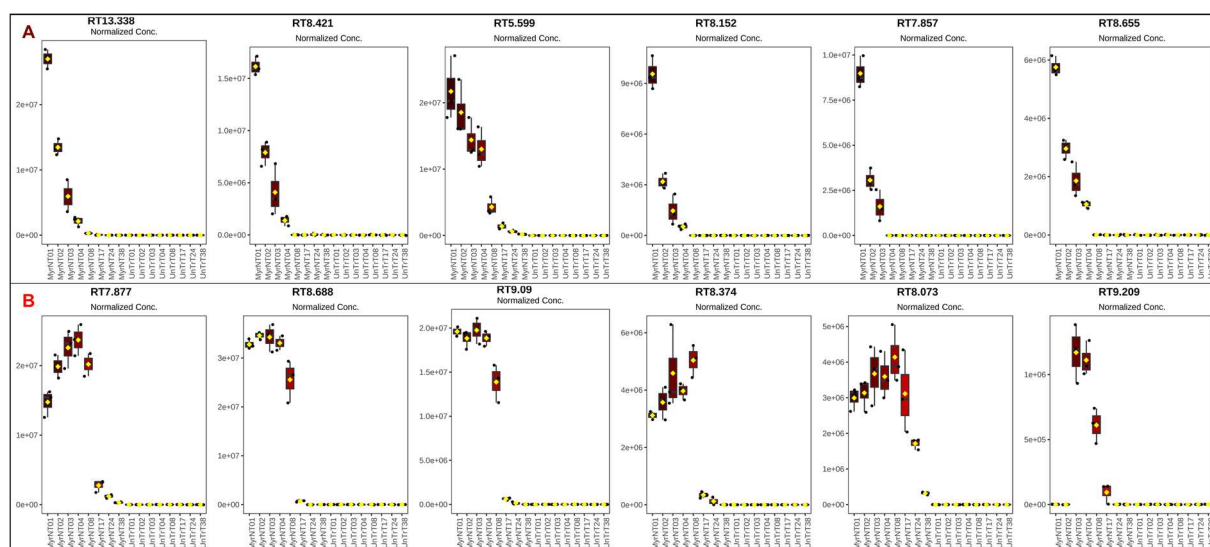


Figure 5

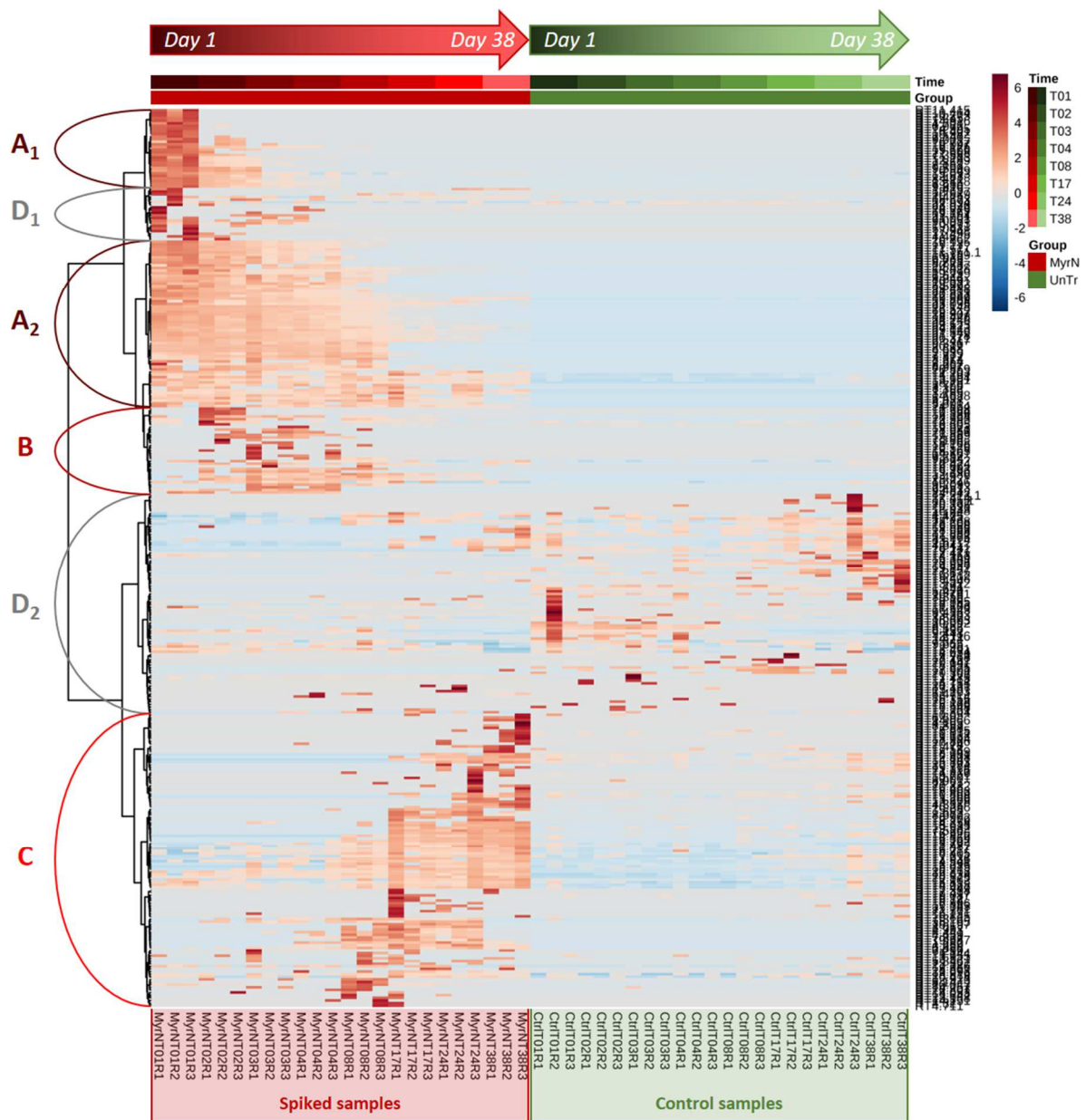


Figure 6

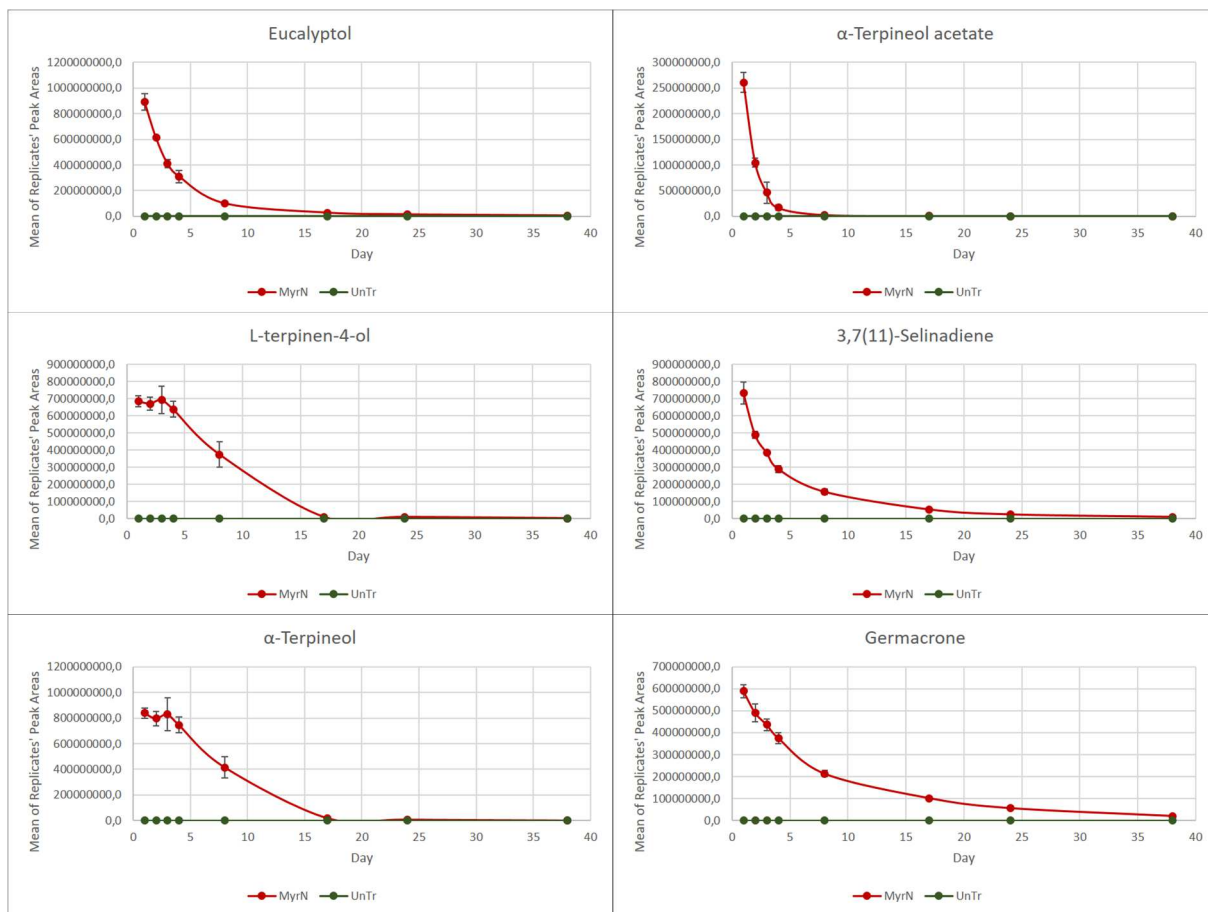


Figure 7

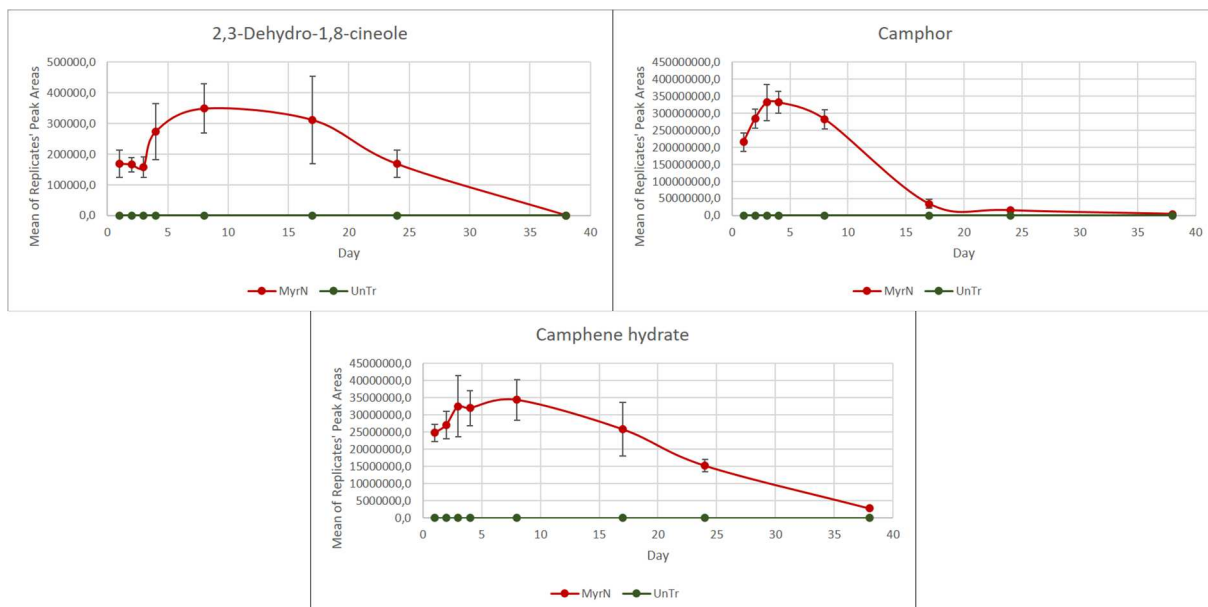


Figure 8

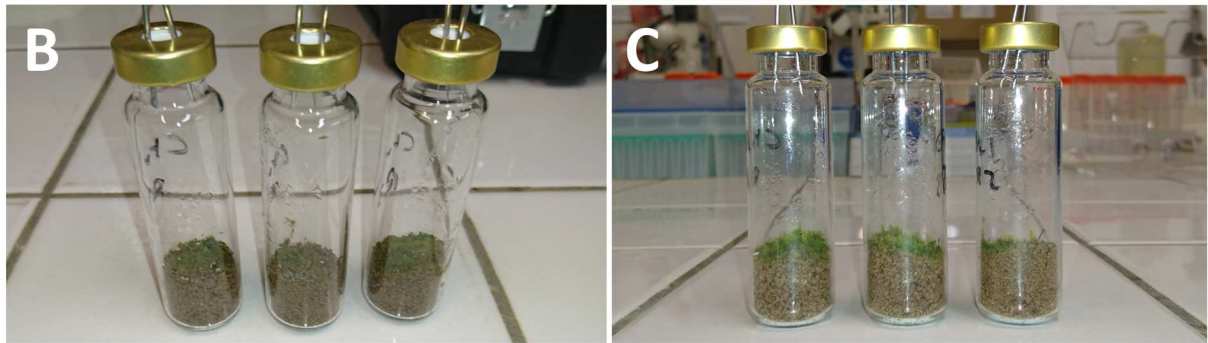
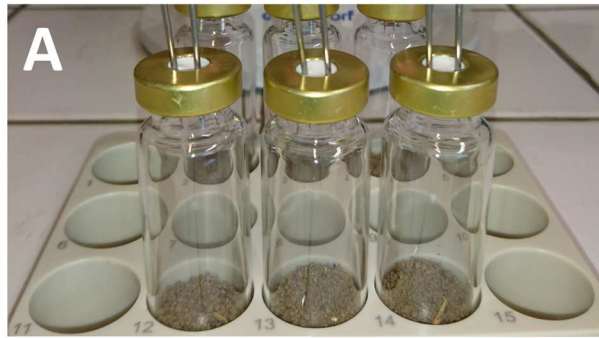


Figure 10

Compound given-code [†]	Putative identity [‡] (level 2 or 3 of identification confidence)	MF	RI (Experimental)	RI (NIST)	Relative intensity (%) [‡]	Reference
<i>Myrica gale methanolic extract components</i>						
RT5.492	p-Cymene	881	1026	1025 ± 2	1.56	[28–30]
RT5.501	o-Cymene	902	1029	1022 ± 2	1.46	N/A
RT5.599	Eucalyptol	910	1036	1032 ± 2	11.09	[28–30]
RT8.421	Borneol	903	1172	1166 ± 7	1.25	[30]
RT8.688	L-terpinen-4-ol	934	1179	1182 ± 0	7.09	[29,30]
RT9.090	α-Terpineol	913	1193	1189 ± 2	7.94	[29,30]
RT11.233	Methyl hydrocinnamate	928	1267	1279 ± 2	1.28	N/A
RT11.751	2-Undecanone	922	1285	1294 ± 2	1.60	[28]
RT13.338	α-Terpineol acetate	934	1342	1350 ± 3	4.75	[30]
RT17.570	Aromadendrene, dehydro-	784	1466	1464 ± 1	5.74	N/A
RT18.448	(+)-β-Selinene	853	1488	1486 ± 3	2.49	[30]
RT18.573	α-Selinene	904	1492	1494 ± 3	1.70	[30]
RT19.299	β-Cadinene	850	1516	1518 ± 10	3.90	[29]
RT20.047	γ-Selinene	907	1541	1544 ± N/A	8.30	N/A
RT20.170	3,7(11)-Selinadiene	913	1547	1542 ± 3	5.96	[28]
RT21.778	Aristolene epoxide	817	1585	N/A	2.84	N/A
RT22.148	cis-β-Elementone	905	1595	1593 ± 3	1.42	[29,30]
RT23.095	1,4-Benzenedipropanol, α,α',γ,γ,γ',γ'-hexamethyl-	710	1622	N/A	1.81	N/A
RT25.500	Germacrone	930	1691	1693 ± 3	5.81	[28–30]
<i>Degradation by-products</i>						
RT2.425	Methyl isovalerate	831	777	773 ± 5	0.04	N/A
RT3.050	Tyranton	834	843	838 ± 8	<0.01	N/A
RT4.259	Butanoic acid, 2,2-dimethyl-3-oxo-, methyl ester	800	946	936	N/C	N/A
RT4.333	Methyl 2-methylhexanoate	770	952	953 ± 2	N/C	N/A
RT4.441	Camphene	932	957	952 ± 2	0.02	[29,30]
RT4.459	β-Pinene	678	960	979 ± 2	<0.01	[29,30]
RT4.953	2,3-Dehydro-1,8-cineole	819	991	991 ± 2	<0.01	N/A
RT6.690	Methyl 2-propylheptanoate	720	1096	1155 ± N/A	N/C	N/A
RT6.885	3-Acetyl-2,5-dimethylfuran	590	1101	1099 ± 4	0.01	N/A
RT7.536	Methyl octanoate	584	1133	1126 ± 2	N/C	N/A
RT7.877	(+)-Camphor	932	1148	1143 ± 9	2.80	[28]
RT8.073	Camphene hydrate	870	1155	1148 ± 2	0.31	[28]
RT8.140	3-Isopropyl-2-methylcyclopentanone	715	1157	1174 ± N/A	N/C	N/A
RT8.267_2	cis-p-Menthan-3-one	809	1164	1164 ± 6	0.35	N/A
RT8.677	2(3H)-Benzofuranone, hexahydro-3a,7a-dimethyl-, cis-	729	1182	N/A	N/C	N/A
RT9.209	Tetrahydrocarvone	856	1200	1208 ± N/A	0.01	N/A
RT11.495	8,9-Dehydrothymol methyl ether	733	1281	1247 ± N/A	0.02	N/A
RT12.486	5-Methoxy-4,4,6-trimethyl-7-oxabicyclo[4.1.0]heptan-2-one	645	1314	N/A	N/C	N/A
RT16.983	Selinan	621	1450	1476 ± 12	0.01	N/A
RT20.371	3,5,11-Eudesmatriene	859	1547	1495 ± N/A	1.92	N/A

Table 1

Compound	Retention Time (min)	PA RSD (%) “Inter-samples” (n = 3)	RT SD (sec) “Inter-samples” (n = 3)	RT SD (sec) “Inter-days” (n = 8)
Eucalyptol	5.60	6.79	0.25	1.61
L-terpinen-4-ol	8.69	4.20	0.18	1.00
α-Gurjunene	17.17	5.34	0.36	0.92
3,7(11)-Selinadiene	20.17	7.75	0.18	2.53
Germacrone	25.50	2.86	0.43	3.44

Table 2

Applied dose (the field dose)	p1			o1			T-test (-Log ₁₀ [p-Value])	
	<i>R2X</i>	<i>R2Y</i>	<i>Q2</i>	<i>R2X</i>	<i>R2Y</i>	<i>Q2</i>	<i>Total TIC area</i>	<i>Number of Molecular Features</i>
20-times	70.30	99.90	98.30	07.68	00.09	00.28	*** 3.67	*** 5.48
10-times	69.40	100.00	98.30	07.64	00.02	00.45	*** 3.93	*** 6.54
1-time	56.60	99.80	94.80	12.70	00.21	00.97	** 3.15	*** 3.49
10 ⁻¹ -time	44.60	99.40	88.50	16.30	00.55	03.76	*** 3.51	** 2.57
10 ⁻² -time	26.20	84.80	48.30	24.30	14.00	11.10	0.70	1.19
10 ⁻³ -time	26.40	75.00	43.60	24.50	24.30	00.43	0.60	0.42

Table 3